A Novel Small-World Model: Using Social Mirror Identities for Epidemic Simulations

Chung-Yuan Huang
Department of Computer and Information Science
National Chiao Tung University and
Department of Computer Science and Information Engineering
Yuanpei Institute of Science and Technology
Hsinchu, Taiwan, Republic of China
gis89802@cis.nctu.edu.tw

Chuen-Tsai Sun
Ji-Lung Hsieh
Department of Computer and Information Science
National Chiao Tung University
1001 Ta Hsueh Road
Hsinchu 300, Taiwan, Republic of China

Yi-Ming Arthur Chen
Institute of Public Health
National Yang-Ming University
155, Section 2, Li-Nong Street
Taipei 112, Taiwan, Republic of China

Holin Lin
Department of Sociology
National Taiwan University
1, Section 4, Roosevelt Road
Taipei 106, Taiwan, Republic of China

The authors propose a small-world network model that combines cellular automata with the social mirror identities of daily-contact networks for purposes of performing epidemiological simulations. The social mirror identity concept was established to integrate human long-distance movement and daily visits to fixed locations. After showing that the model is capable of displaying such small-world effects as low degree of separation and relatively high degree of clustering on a societal level, the authors offer proof of its ability to display R_0 properties—considered central to all epidemiological studies. To test their model, they simulated the 2003 severe acute respiratory syndrome (SARS) outbreak.

Keywords: Social mirror identity, small-world network model, multiagent system, cellular automata, public health policy, network-based epidemic simulations

1. Introduction

Factors that influence the transmission dynamics of epidemics include individual diversity and social networks constructed by interpersonal relationships and simple daily contact [1-6]. For instance, interactions among individuals and contact routes both affect the outbreak of short-distance contagious diseases such as severe acute respiratory syndrome (SARS) and enteroviruses [3, 5-11]. Due to the potential complexity of human interactions, researchers need a simulation model that can represent multiple social networks to analyze and control a wide range of potential transmission behaviors and epidemic characteristics.

SIMULATION, Vol. 81, Issue 10, October 2005 xxx-xxx

DOI: 10.1177/0037549705061519

Furthermore, epidemic transmission speed and scope are closely related to daily human activities. Modern lifestyles are marked by strong habits with little day-to-day variety. For instance, the majority of adults in developed countries use the same transportation modes for short- and long-distance movement on a daily basis. The limited diversity of transportation options to sites that are visited regularly (e.g., workplaces and schools) makes it easy for the rapid transmission of diseases within a town or city. Since it is hard to control the movement of individuals (e.g., method, timing, direction, and distance), researchers are repeatedly challenged by the task of simulating individual movement within a society—an issue referred to in the literature as the "mobile individual problem" [12-15].

Researchers who use small-world network models to investigate epidemics usually divide human contacts into short-distance (short-link) and long-distance (long-link) contact categories [1-6, 16-19]. While these models offer partial explanations for the mobile individual phenomenon, they fail to accurately express concurrent epidemic movement from one infectious agent to a group of susceptible people—for instance, coworkers, classmates, hospital employees, or passengers taking the same bus. When applying small-world network models to epidemics, indirect descriptions such as shortcuts and short/long or strong/weak links may not accurately reflect the repeated use of transportation tools for long-distance movement and for visiting multiple sites in one day. For this reason, epidemiologists, public health specialists, and health authorities cannot use most of the abstract small-world network models that have been proposed to test the efficacy of various public health policies and epidemic prevention strategies.

In this article, we propose a social mirror identity concept that accurately reflects human interaction (including long-distance movement and daily visits to fixed and/or multiple locations) in modern societies (Fig. 1). According to the social mirror identity concept, every visited location, every played role, and every performed activity is considered a social mirror identity of the individual in question. A list of one's social mirror identities might include father, husband, coworker, supervisor, subordinate, fellow passenger, store customer, or restaurant diner. Each role or activity at each location is considered a separate mirror identity. The mirror identity concept allows for a more complete and direct imitation of social phenomena and daily movement. In combination with cellular automata, we offer it as a solution to the mobile individual problem.

2. Related Epidemiological Models and Concepts

2.1 Compartmental Models

Many epidemiologists have used compartmental models to predict epidemic outbreak trends [20, 21]; the most basic and well known is the SIR model created by William Kermack in 1927 (Fig. 2) [20]. During the 2002-2003 SARS outbreaks, many researchers used compartmental models to estimate transmission dynamics and developmental tendencies [22-26] and to analyze super-spreader events (SSEs). However, those models were only capable of calculating change in the total number of infected individuals per time step. During each simulation, differential equations were applied to calculate pivotal parameters, including the basic case reproduction number R_0 [27, 28], which is considered essential to the work of public health specialists and epidemiologists. To generate more accurate simulation results, some researchers divided each population into subgroups according to age, location of residence, infection rate, and other characteristics of interest to epidemiologists [22-23, 26]. Regardless of characteristic or category, these simulation models ignore the fact that social phenomena emerge from regular and frequent human interaction. In other words, compartmental models emphasize epidemic characteristics (e.g., transmission, mortality, and recovery rates) at the expense of population structure, social space, heterogeneity, localization, and interaction. Consequently, compartmental models are insufficient for analyzing public policy issues and epidemic prevention strategies.

The basic case reproduction number R_0 is an index parameter with an important reference value—the number of people infected by a patient prior to recovery or death. When R_0 is greater than 1, the number of infected patients increases, and the transmission rate soars. An R_0 of 1 indicates stability in the spread of the infection—in other words, each patient transmits the virus to one person on average. When R_0 is smaller than 1, a patient may or may not transmit the virus, making the recovery rate higher than the infection rate. Accordingly, 1 is considered a plague threshold value; to prevent an epidemic from becoming a plague, R_0 must remain below the threshold value.

2.2 Simple Social Network Models

There are at least two ways of constructing a simple network model:

1. *Lower dimensional lattices* that represent social networks (Fig. 3a) [14, 29, 30]. Examples include one-dimensional ring-shaped lattices and two-dimensional lattices with periodic boundary conditions (i.e., a doughnut-shaped surface). Since each node is connected to its adjacent nodes and the number of connected nodes never changes, these models are sometimes referred to as regular network models.

2. *Random networks* that represent social networks (Fig. 3b) [31]. This type of network model and the compartmental model described above are equivalent in that both use statistics to represent many social network characteristics. Random network models are considered primitive means of representing complex, chaotic, and unpredictable societies.

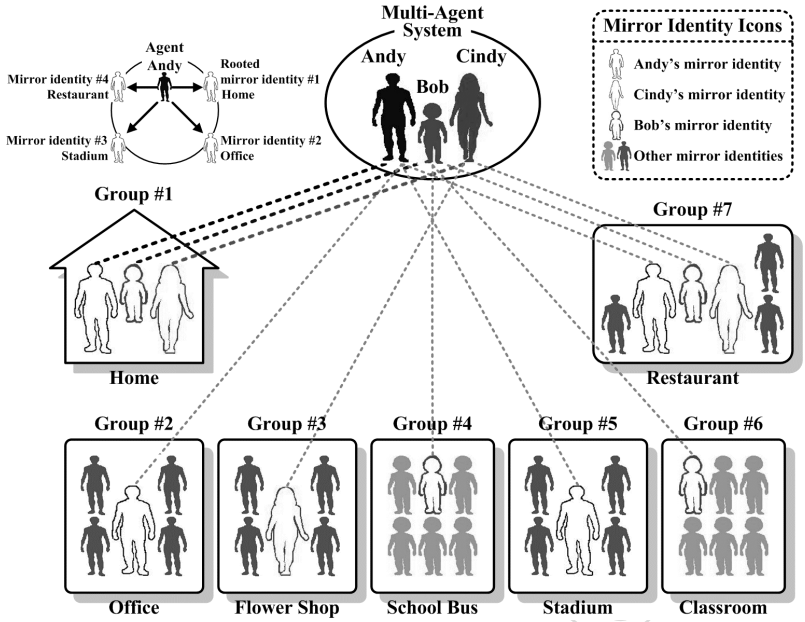

Figure 1. An example of the social mirror identity concept

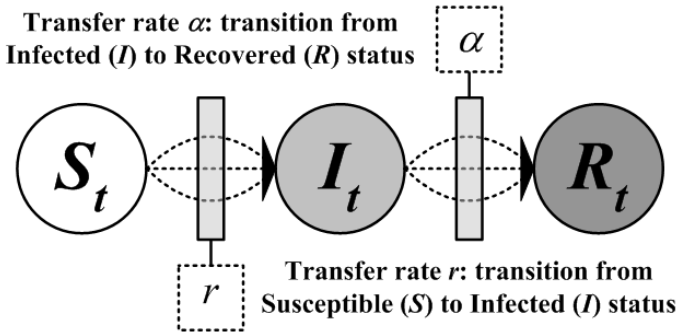

Figure 2. General transfer diagram for the compartmental SIR model with susceptible population S, infected population I, and recovered population R

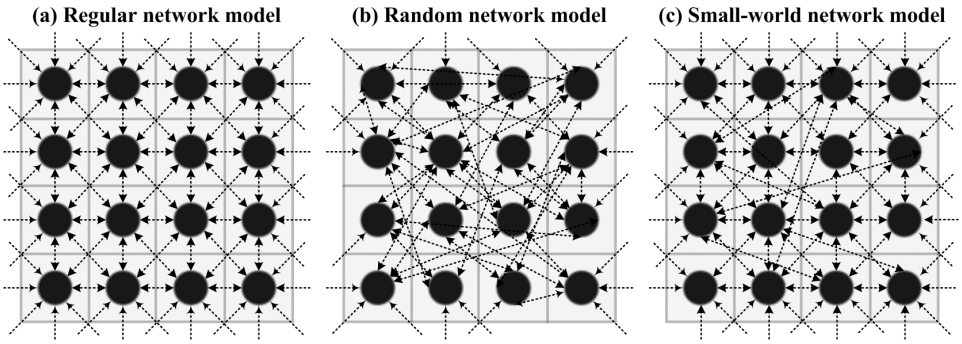

Figure 3. Social network models: (a) regular, (b) random, and (c) small world

In either model, communities, cities, and countries can be defined as separate social networks; even our planet can represent one social network. One node represents one individual with status-determining attributes, for example, epidemiological progress, gender, age, or immunization. Connections between individuals are referred to as edges, with different edges representing different interpersonal relationships. Edges in AIDS simulations represent sexual relationships, while in SARS simulations, they represent close physical proximity. The states of all network nodes change simultaneously during each time step. The state of each individual node is determined by its original state, its neighbor's state, and a set of interaction rules.

Some researchers have used two-dimensional cellular automata to explore local transmission mechanisms and epidemic characteristics [30, 32-37]. Cellular automata are considered specific and regular network models. They exhibit social properties such as population structure, local aggregation, social space, heterogeneity, and interaction—all of which are essential to understanding epidemiological and contagion issues (Fig. 4). They are useful for observing disease transmission during an epidemic, but they lack an important network property—small-world phenomenon—meaning that they generally fail to represent low degrees of separation among individuals [18]. Without this property, a social network model cannot accurately simulate real transmission dynamics or modern public health policies associated with epidemic diseases.

2.3 Small-World Social Network Models

2.3.1 Triadic Closure

First proposed by Rapoport [38] in 1957, the triadic closure concept is based on the view of human beings as "birds of a feather." Accordingly, employees in the same company, classmates in the same school, and regular customers at a coffee shop have a much better chance of meeting each other and forming relationships than two strangers. In other words, relationships are formed because of what people have in common, not because of random probabilities. The triadic closure concept posits that two strangers with a common friend have a higher than average probability of meeting each other and becoming friends themselves. Triadic relationships are thus viewed as a fundamental structural unit, complete with social rules governing connections among individuals. Connections established via multiple triads form large social networks. Whenever an epidemic outbreak occurs, healthy but susceptible locals are most likely to become infected due to their triadic and/or polygonal closure relations with infectious patients.

2.3.2 Small-World Network Models

While working on his well-known letter delivery experiment in 1967, Milgram [39] proposed a concept called "six degrees of separation" to explain the phenomenon in which humans frequently interact with each other and form groups, yet everybody in the world remains separated by only six other people. Milgram's idea was verified in 1998 by Watts and Strogatz [16] (Fig. 3c). Their small-world network model (which contains the characteristics of high clustering and low degree of separation) was based on two concepts: (1) topological networks and structures are ubiquitous in the real world, and (2) they strongly influence social issue dynamics and outcomes [5, 17-19, 40]. Because of their work, the capability of any social simulation model to portray high clustering and low degree of separation is now considered an important index for examining social network models. Social individuals are characterized by long-distance movement, daily visits to fixed locations, multiple activity locations, and local clustering—meaning that the average distance between any two individuals is shortened. Geographic location and distance are therefore considered secondary causal factors in epidemic outbreaks.

2.3.3 The Small-World Phenomenon

Determining whether a social network model is indeed a small-world network model requires validation of a high clustering coefficient and a low degree of separation coefficient. A clustering coefficient is used to evaluate the degree of connection between two neighboring nodes. In equation (1), graph G represents a social network, v_i is a node in graph G, and k_i is the vertex degree of node v_i. The $C(v_i)$ clustering coefficient of node v_i is defined as the ratio of E_i (the number of edges that actually exist among the k_i nodes) and $k_i \times (k_i - 1)/2$. Accordingly, the $C(G)$ clustering coefficient of the entire social network equals the average $C(v_i)$ value for all nodes.

$$C(v_i) = \frac{2 \times E_i}{k_i \times (k_i - 1)}. \quad (1)$$

The $S(v_i, v_j)$ separation coefficient is used to evaluate the shortest distance between two random nodes, v_i and v_j. The $S(G)$ separation coefficient of the entire social network is the average length of the shortest distances between any two nodes. When the number of individuals in a society increases, the average separation coefficient between any two individuals increases logarithmically rather than proportionally [17].

3. The Proposed Model

As shown in Figure 5, our simulation model consists of two layers. The upper layer is a simplified multiagent system for simulating heterogeneous cohorts, and the lower layer contains two-dimensional $n \times n$ cellular automata that represent real-world activity spaces. Social mirror identities are used to connect the two layers, thus establishing a small-world network model. By manipulating transmission rules, disease parameters, and public health policies, the model can be used to simulate the transmission dynamics of contagious diseases, verbal communication, and social issues.

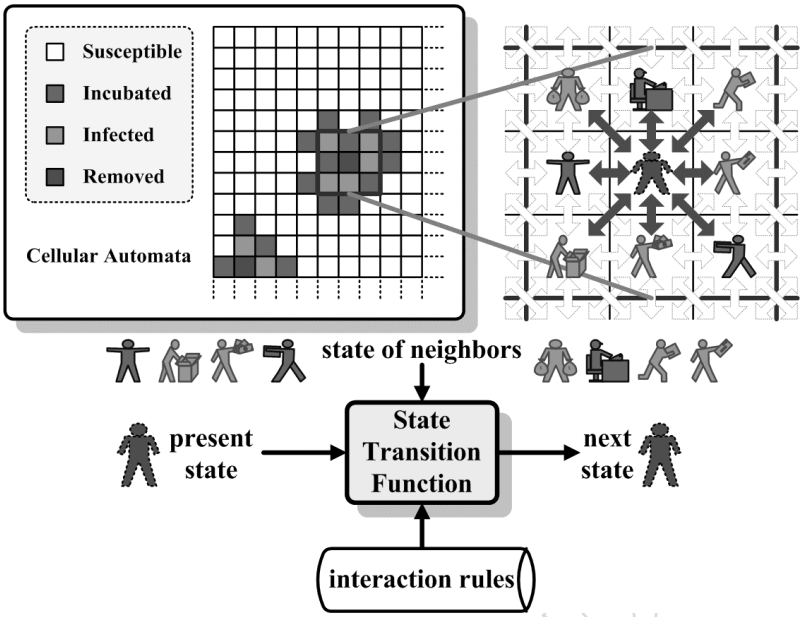

Figure 4. Cellular automata and state transition function

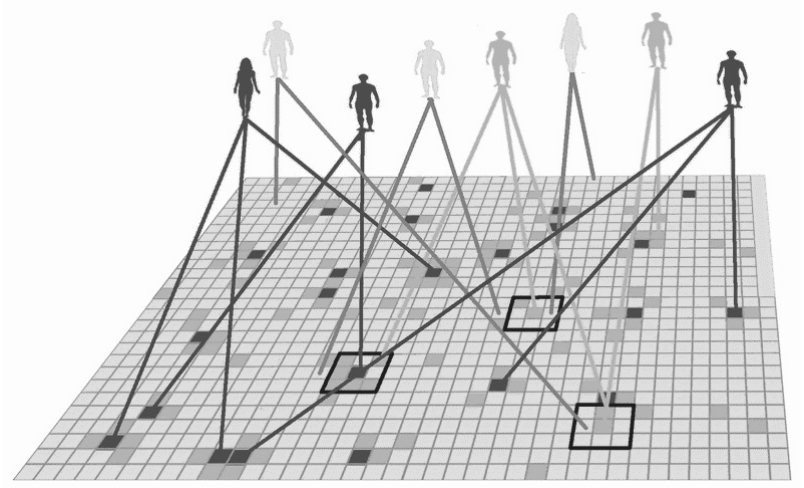

Figure 5. Cellular automata with the social mirror identity model (CASMIM)

3.1 Cellular Automata with Social Mirror Identities Model (CASMIM)

In the cellular automata with social mirror identities model (CASMIM), each individual is depicted as a single agent in the upper-layer multiagent system, and the places that an agent visits on a regular basis (e.g., homes, train stations, workplaces, and restaurants) are defined as that individual's social mirror identities. In typical cellular automata, lattices represent abstract agents. In our model, each lower-layer cellular automata lattice represents a social mirror identity.

It is possible for multiple social mirror identities to be connected to the same agent. Each agent has many social mirror identities representing fixed locations that are visited daily or very frequently. The number of social mirror identities connected to any single agent exhibits a normal distribution. Small clusters formed by a mirror identity and its neighbors can represent family members, coworkers, fellow commuters, health care workers, relatives in

hospitals, or diners in restaurants. The mirror identity concept uses simple social networks to preserve the properties of elements that interact with their neighbors within two-dimensional lattices and to reflect such activities as long-distance movement and daily visits to fixed locations.

In the example shown in Figure 1, Andy spends 1 hour every morning taking his wife Cindy to her job at a flower shop before driving to his insurance company office. Their son Bob takes a school bus to his elementary school. At least once a week, the three of them eat dinner at their favorite restaurant. After dinner, Andy often takes Cindy and Bob home before going with his friends Dick, Eric, and Frank to watch a baseball game. According to our proposed model, Andy, Bob, Cindy, Dick, Eric, and Frank are upper-layer agents, and Andy's home and office and the restaurant and stadium are lower-layer mirror identities. Bob's mirror identities are his home, school bus, classroom, and the restaurant. Cindy has only three mirror identities: home, the flower shop, and the restaurant. Andy's automobile is considered an extension of their home node rather than a separate activity node since Andy rarely uses it to transport anyone outside of his family. Bob's school bus is considered a social mirror identity because he uses it 5 days per week and plays with many of the children who take the same bus.

Each individual upper-layer agent has a set of attributes that demonstrate its epidemiological progress and social mobility status (Table 1, Fig. 6); all of the agent's social mirror identities have access to these attributes. In addition, each social mirror identity has a group of private attributes that represent its current status, location, and special activity locations—homes, hospitals, or dormitories (Table 2). Agents who possess individual social mirror identities have complete access to these attributes. In the Figure 1 example, Andy belongs to one group at home with Cindy and Bob, a second group at his office with his coworkers, a third group (also with Cindy and Bob) with other customers at their favorite restaurant, and a fourth group with his baseball friends. Andy's social mirror identities form a star-shaped topology, with Andy at the center and the mirror identities at the vertices.

According to our proposed model, the greater the number of social mirror identities an agent has, the greater the agent's influence. In epidemiological terms, the more social mirror identities an agent has, the more likely the agent will become infected or transmit a disease to other agents. In cellular automata terms, the lattices surrounding a social mirror identity represent neighbors, family members, classmates, colleagues, friends, hospital workers, passengers on the same bus, customers in the same restaurant, and so on. Andy's lower-layer social mirror identity at the baseball stadium is adjacent to those of Dick, Eric, and Frank, and his lower-level social mirror identity at home is adjacent to those of Cindy and Bob.

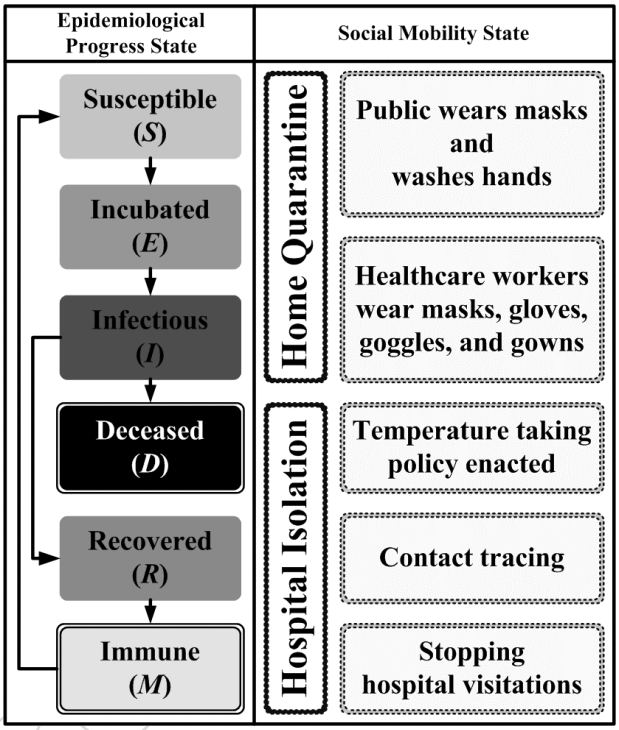

Figure 6. Epidemiological and social mobility states

We decided to use the Moore neighborhood concept with a radius parameter of 1 (Fig. 7) in CASMIM because von Neumann neighborhoods lack triadic closure relationships between a lattice and its four neighboring lattices. In contrast, each lattice in a Moore neighborhood has triadic closure relationships with its eight neighboring lattices; this higher degree of local clustering matches Rapoport's description of interactions in human societies. In the Figure 1 example, if Andy catches the flu from his friend Dick, he may infect his wife and son. According to triadic closure relationships, there is a high probability that Bob, Eric, and Frank will also become infected.

With a few important exceptions (e.g., AIDS), most epidemic simulation models assume that one time step is equivalent to one 24-hour period in the real world. We used that assumption when designing CASMIM. As shown in Figure 8, the statuses of upper-layer agents change simultaneously with their lower-layer social mirror identity statuses during each time step. Each agent's social mirror identity comes into contact with all of its surrounding neighbors' social mirror identities in random order per time step; contact order is not considered critical. The attributes of the social mirror identity, the agent, and other associated social mirror identities vary according to the attributes of the social mirror identities of neighboring agents, a set of

Table 1. Agent attributes

Attribute	Data Type	Description	Default Value
ID	Integer	Unique serial number that identifies agent in CASMIM.	1∼ P
E	Symbol	$Rate_{Forever Immune}$ determines proportion of agents classified as M (Immune) in the epidemiological progress attribute E (i.e., the population of permanently immune agents). All other agents are classified as S (Susceptible)—"not yet infected but prone to infection."	Susceptible, Immune
Mobility	Symbol	Default value is "free"—no restrictions on interacting with the mirror identities of neighboring agents. When an agent is placed under home quarantine or hospital isolation, its *Mobility* status changes to *Quarantined* or *Isolated*, meaning that the agent is restricted to its rooted social mirror identity (home, hospital, or dormitory) and that the activities of all social mirror identities are temporarily suspended.	Free
Count	Integer	Records the number of an agent's mirror identities; each agent has a minimum of 1 and a maximum of M. The number of an agent's mirror identities exhibits a normal distribution.	1∼ M
MirrorIdentity	Set	Data structure for containing mirror identities.	
Age	Symbol	Agents are categorized as young (1 to 20), prime (21 to 60), and old (61 and above). Ages are randomly assigned according to $Rate_{Young}$, $Rate_{Prime}$, and $Rate_{Old}$ parameters.	Young, Prime, Old
Super	Boolean	Denotes whether an agent is a super-spreader. If yes, set *Super* to "true"; if no, to "false." The $Rate_{Super}$ parameter determines which agents are super-spreaders.	True, False
Immunity Permanent	Boolean	Denotes whether an agent is permanently immune. If yes, set *ImmunityPermanenty* to "true"; if no, to "false." The $Rate_{Forever Immunity}$ determines which agents are permanently immune.	True, False
Day	Integer	Number of days for each of the three epidemiological progress states. If an infected agent has not yet recovered, *Day* is used to indicate the number of infected days. For recovered agents, *Day* is used to indicate the number of days since full recovery. If a recovered agent has temporary antibodies, *Day* is used to indicate the number of immune days.	
$Rate_{Contact}$	Real	Rate of contact with other agents. For all agents, $Rate_{Contact}$ values exhibit a normal distribution.	0∼1
WearingMask	Boolean	Denotes whether an agent wears a mask. If yes, set *WearingMask* to "true"; if no, to "false." Default value is "false." When a mask-wearing policy is enacted (for the general public or for health care workers), the $Policy_{WearingMask}.Parameter.Rate_{Participation}$ parameter is used to determine how many agents wear masks.	False
MaskType	Real	Average prevention grade of agent masks. The higher the number (closer to 1), the greater the efficacy.	0∼1
$Quarantined_{Day}$	Integer	Number of home quarantine days, with a range of 0 to $Policy_{HomeQuarantine}.Parameter.Day_{Quarantined}$.	

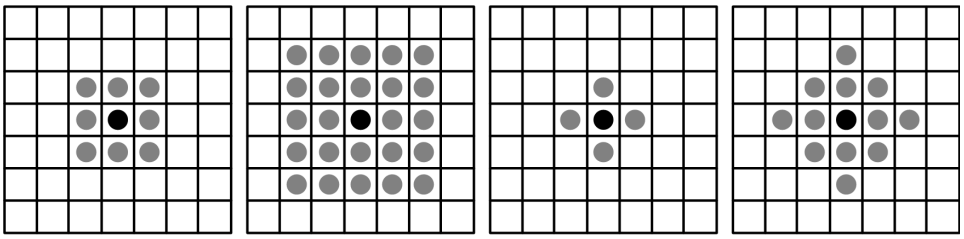

Figure 7. Examples of von Neumann and Moore neighborhoods

Table 2. Social mirror identity attributes

Attribute	Data Type	Description	Default Value
Root	Boolean	Each agent has one mirror identity whose *Root* = true; for all other mirror identities, *Root* = false. The rooted mirror identity is used to mimic special activity locations—for instance, homes, hospitals, and dormitories.	True, False
Suspend	Boolean	Default value is false for all mirror identities, denoting that they can move about without restriction. Except for rooted mirror identities, *Suspend* = true for all mirror identities of an agent in home quarantine or hospital isolation, representing the idea that the agent cannot interact with other adjacent neighbors outside of its home or hospital until the end of the quarantine or recovery period. If the agent dies, *Suspend* = true for all mirror identities (including rooted mirror identity), representing the idea that the agent can no longer visit any other location.	False
Location	(Integer, Integer)	The first number represents the x-axis coordinate and the second the y-axis coordinate for the location of a mirror identity in the two-dimensional cellular automata. Each mirror identity is mapped to a single coordinate location; in other words, each coordinate location contains a single mirror identity of only one agent.	
Neighbor	Set	Represents the coordinate locations of mirror identities of neighboring agents. We adopted the Moore neighborhood definition for our simulation model. Under this neighborhood structure, each mirror identity is defined as having eight neighbors.	

interaction rules (to be described in section 4), simulation and epidemic disease parameters (Table 3), public health policy parameters (Table 4), and probabilistic causes (e.g., symptom detection rate).

At this point, our simulation model is considered a small-world social network model with such simple social network attributes as population structure, area clustering, space, heterogeneity, localization, and interaction. It also has the social attributes of long-distance movement, daily visits to fixed locations, multiple activity nodes, and the small-world characteristic of low degree of separation—all of which are suitable for simulating epidemics, communication networks, and other contagion problems. Moreover, one advantage of CASMIM is its use of the social mirror identity concept to reflect individual geographic mobility in special areas; this characteristic is particularly useful for analyzing public health policies.

3.2 Implementing CASMIM

Our simulation system (created with C++) consists of many functional modules, including CASMIM, an epidemiology module, a social mobility module (e.g., families, dormitories, and hospitals), and a public health policy module. We created a general-purpose and extendable software platform that is suitable for detailed numerical experimentation and classroom demonstrations of specific epidemic diseases and public health policy suites. The computational flowchart and system architecture for our proposed simulation system are shown in Figures 8, 9, and 10, respectively.

To accommodate different requirements, we applied the visual component library (VCL) and event-driven programming model that is part of the Borland C++ Builder to design the user interface and various input/output functions of the simulation system (Fig. 11). In addition to providing many specific statistical reports and charts on epidemic data, the simulation system offers two browser windows (micro-view and macro-view) to observe real-time epidemic disease infection situations in an agent society. After complied using the Borland C++ compiler and conversion into an executable application, the simulation system can be run on Windows with Dynamic Linked Library (DLL) files. Our simulation system is available at ftp://anonymous@140.126.75.253; for source code on particular contagious diseases or specific research requirements, please contact the authors.

As shown in Figure 12a, the CASMIM construction process consisted of four steps, with each step using its respective subprocedure to initialize the data structures and to establish relations among these data objects. The four steps were as follows: (1) call the initialize-multiagent-system subprocedure to initialize the upper-layer multiagent system, as shown in Figure 12b; (2) call the initialize-cellular-automata subprocedure to initialize the lower-layer cellular automata, as shown in Figure 12d; (3) call the distribute-mirror-identities-to-CA subprocedure to distribute all of an agent's social mirror identities to cellular automata lattices so that the upper-layer multiagent system and lower-layer cellular automata connect with each other, thus establishing one-to-one mapping; and (4) call the set-rooted-mirror-identities-of-all-agents subprocedure to define all of an agent's rooted mirror identities (subprocedure applications are discussed in section 4.2). For default

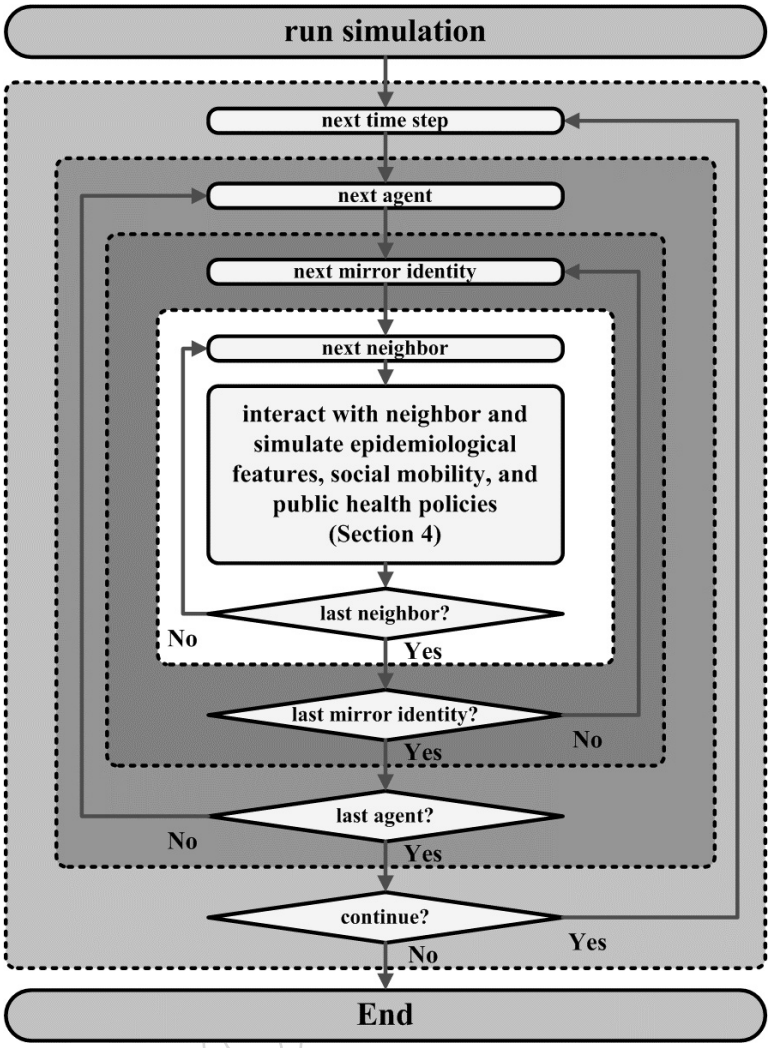

Figure 8. Simulation flowchart

values and related explanations of agent and social mirror identity attributes, see Tables 1 and 2; for system parameters used by agents, social mirror identities, and cellular automata during the initialization process, see Table 3.

The initialize-multiagent-system subprocedure repeats four additional steps until all agents are initialized, at which time it returns to the create-CASMIM procedure. The four steps are as follows: (1) selecting an un-initialized agent from the agent population, (2) giving the agent an ID, (3) initializing the agent's attributes, and (4) calling the initialize-agent-mirror-identities subprocedure to initialize the data structure used by the agent to contain its social mirror identities (Fig. 12c).

The initialize-cellular-automata and initialize-multiagent-system execution processes are very similar. According to the row-major layout, the attributes of each cellular automata lattice are initialized from top to bottom row and from left to right column. The initialize-agent-mirror-identities process is even more basic; it repeatedly executes two steps for every social mirror identity of an agent: it gives the identity a serial number and initializes its attributes (Table 2). Accessing the private attributes of a social mirror identity requires its serial number and the ID of the agent who possesses the identity.

In CASMIM, since each cellular automata lattice is connected to an agent's social mirror identity, a procedure for lattices and social mirror identities to form one-to-one maps is required in order to provide access to each other's private attributes. A coordinate attribute designated *Location* (x, y) is used by an agent's social mirror identity to

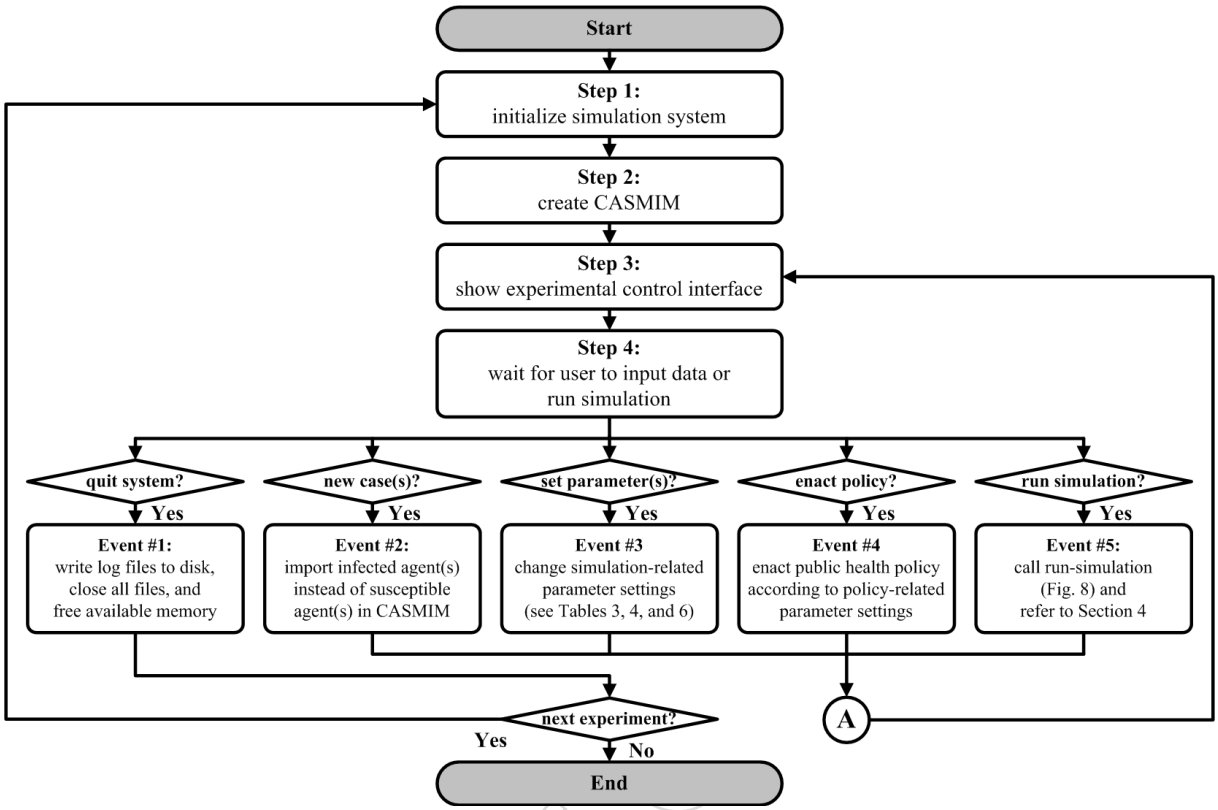

Figure 9. System flowchart

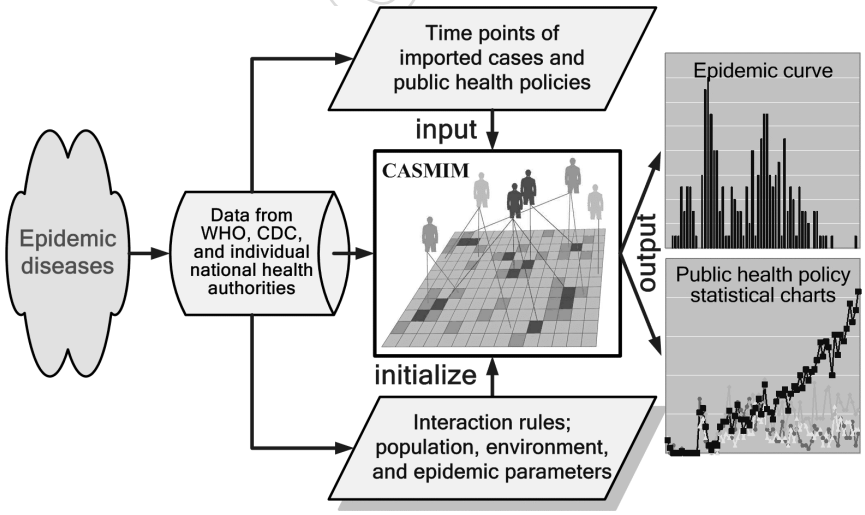

Figure 10. Simulation framework. Data on reported cases were collected from the World Health Organization (WHO) and national health authorities. Input data were categorized as epidemic parameter (e.g., average incubation period, infection rate, distribution among age groups, mortality), imported case (e.g., time point, amount, imported during incubation or illness period), and activated public health policy (e.g., number of quarantine days, efforts to take body temperatures, restricting access to hospitals). Simulation output includes cellular automata states and various statistical charts.

Table 3. Simulation system and epidemic disease parameters

Attribute	Data Type	Description	Default Value
$Population_{Agent}$	Set	Stores total agent population in simulation system.	
P	Integer	Total number of agents.	100,000
M	Integer	Upper limit of an agent's mirror identities.	5
H	Integer	Height of two-dimensional lattice used in cellular automata.	500
W	Integer	Width of two-dimensional lattice used in cellular automata.	500
N	Integer	Total number of usable lattices ($H \times W$) in cellular automata.	250,000
$Period_{Incubation}$	Integer	Average number of incubation days.	5
$Period_{Infectious}$	Integer	Average number of infectious days.	25
$Period_{Recovered}$	Integer	Average number of recovered days.	7
$Period_{Immune}$	Integer	Temporarily immune to the disease.	
$Rate_{Super}$	Real	Percentage of super-spreaders in total population.	0.0001
$Rate_{Young}$	Real	Percentage of young (0 to 20 years) agents in total population.	0.3
$Rate_{Prime}$	Real	Percentage of prime (21 to 60 years) agents in total population.	0.5
$Rate_{Old}$	Real	Percentage of old (60 years and above) agents in total population.	0.2
$Rate_{ForeverImmunity}$	Real	Percentage of permanently immune agents in total population.	
$Rate_{Infection}$	Real	Average infection rate.	0.045
$Rate_{Death}$	Real	Average death rate.	0.204
$Frequency_{Contact}$	Real	Number of contacts between an agent and its neighbors per time step.	4

Table 4. Public health policy parameters

Policy	Attribute	Data Type	Description
WearingMaskInGP	$Rate_{Participation}$	Real	Policy participation rate.
	$Rate_{Prevention}$	Real	Infectious disease prevention rate.
WearningMaskInHW	$Rate_{Participation}$	Real	Policy participation rate.
	$Rate_{Prevention}$	Real	Infectious disease prevention rate.
TemperatureMeasuring	$Rate_{Detection}$	Real	Fever detection success rate.
	$Rate_{Participation}$	Real	Measurement participation rate.
HomeQuarantine	*Class*	Symbol	A- and B-class quarantines.
	$Day_{Quarantined}$	Integer	Number of home quarantine days.
	$Rate_{Participation}$	Real	Policy participation rate.
RestrictedAccessToHospitals	$Rate_{Participation}$	Real	Policy participation rate.
ReducedPublicContact	$Rate_{Participation}$	Real	Policy participation rate.

record its position in the cellular automata. Two private attributes (*MirrorIdentityNo* and *AgentID*) are used by the cellular automata lattice to refer to the social mirror identity and the agent who possesses it. Moreover, the private attributes *Root* and *Suspend* (Table 2) are used to model specific epidemic situations such as home quarantine, hospital isolation, the infectious condition of one's family and neighborhood during a home quarantine, or the infectious condition of health care workers in a hospital where an agent is being held in isolation.

After initializing the upper-layer agent population and lower-layer cellular automata, the distribute-mirror-identities-to-CA subprocedure is called to establish one-to-one mapping between an agent's social mirror identity and the cellular automata lattice. Through this procedure, a small-world network model is created for simulations. The pseudo-code for the distribute-mirror-identities-to-CA subprocedure is

```
procedure distribute-mirror-
identities-to-CA is
  for index i from 1 to
  System.Parameter.P do loop
    Agent_Index(i).Attribute_Limit ←
    random-by-normal-distribution
    (1, System.Parameter.M)
  for index y from 1 to
  System.Parameter.H do loop
    for index x from 1 to
    System.Parameter.W do loop
```

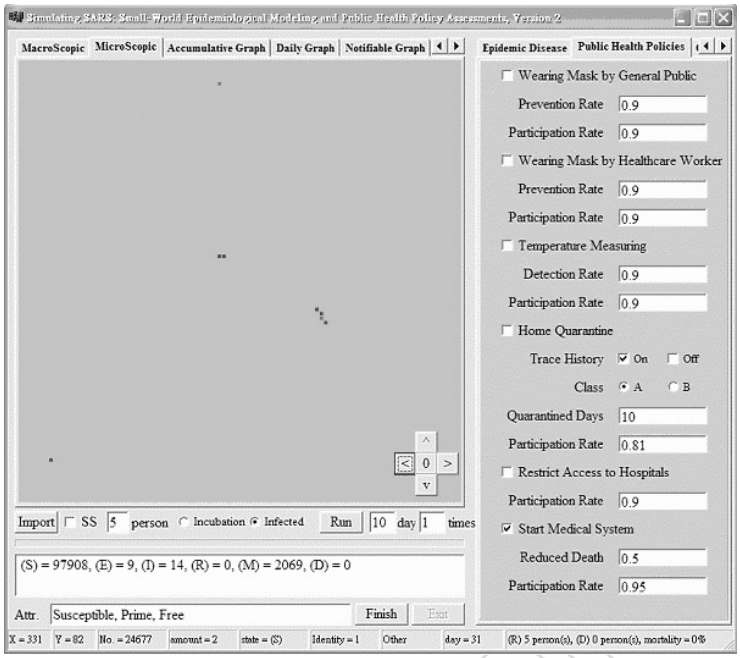

Figure 11. Simulation system for contagious infections

```
    Allocate:
    ID ← random(1, System.
    Parameter.P) // ID ∈ [1, System.
    Parameter.P]
    if Agent_Index(ID).Attribute_Count ≥
    Agent_Index(ID).Attribute_Limit then
     goto Allocate:
    No ← Agent_Index(r).Attribute_Count ←
    Agent_Index(r).Attribute_Count + 1
    call connect-mirror-identity-with-
    cell(ID, No, x, y)
  return

  procedure connect-mirror-identity-
  with-cell (parameter ID, No, x, y) is
    Agent_Index(ID).MirrorIdentity_Index(No).
    Attribute_Location ← coordinates(x, y)
    Environment_CA.Cell_x,y.Attribute_AgentID
    ← ID
    Environment_CA.Cell_x,y.
    Attribute_MirrorIdentityNo ← No
  return
```

This subprocedure consists of two parts. In the first, a random number between 1 and *System.Parameter.M* (Table 3) is generated for each agent, and the number is assigned as the upper limit of possible social mirror identities for an agent. The number of identities should exhibit a normal distribution. In the second part, two methods are used to connect the cellular automata lattices with the agents' social mirror identities. In the first method, each lattice is assigned a randomly chosen agent from top to bottom row and from left to right column, then each agent is connected to an available lattice with a social mirror identity that has yet to form its own lattice connection. If the number of connections between an agent's social mirror identities and lattices has already reached its upper limit, the agent is released and another agent randomly chosen for the same procedure. In the second method, each agent's social mirror identity is assigned to a randomly chosen cellular automata lattice. Determining which method to apply depends on a combination of simplicity and the particular requirements of the epidemic disease being examined.

The polymorphous Index(n) function used in the distribute-mirror-identities-to-CA subprocedure has two calling situations: $Agent_{Index(n)}$, where Index(n) refers to a certain agent with an ID of n, and $Agent_A.MirrorIdentity_{Index(n)}$, where Index($n$) refers to a specific social mirror identity of agent A with an serial number of n. Index(n) has an inverse function designated Trace(S), which also has two calling situations: $Agent_{Trace(S)}$ (which returns the ID of a certain agent S) and $Agent_A.MirrorIdentity_{Trace(S)}$ (which returns the serial number of a specific social mirror identity S of agent A). According to these definitions, it is possible to deduce $Agent_A$ = Index(Trace($Agent_A$)). For examples of function Trace(S), see section 4.1.

After a social mirror identity and lattice are chosen, the distribute-mirror-identities-to-CA subprocedure calls

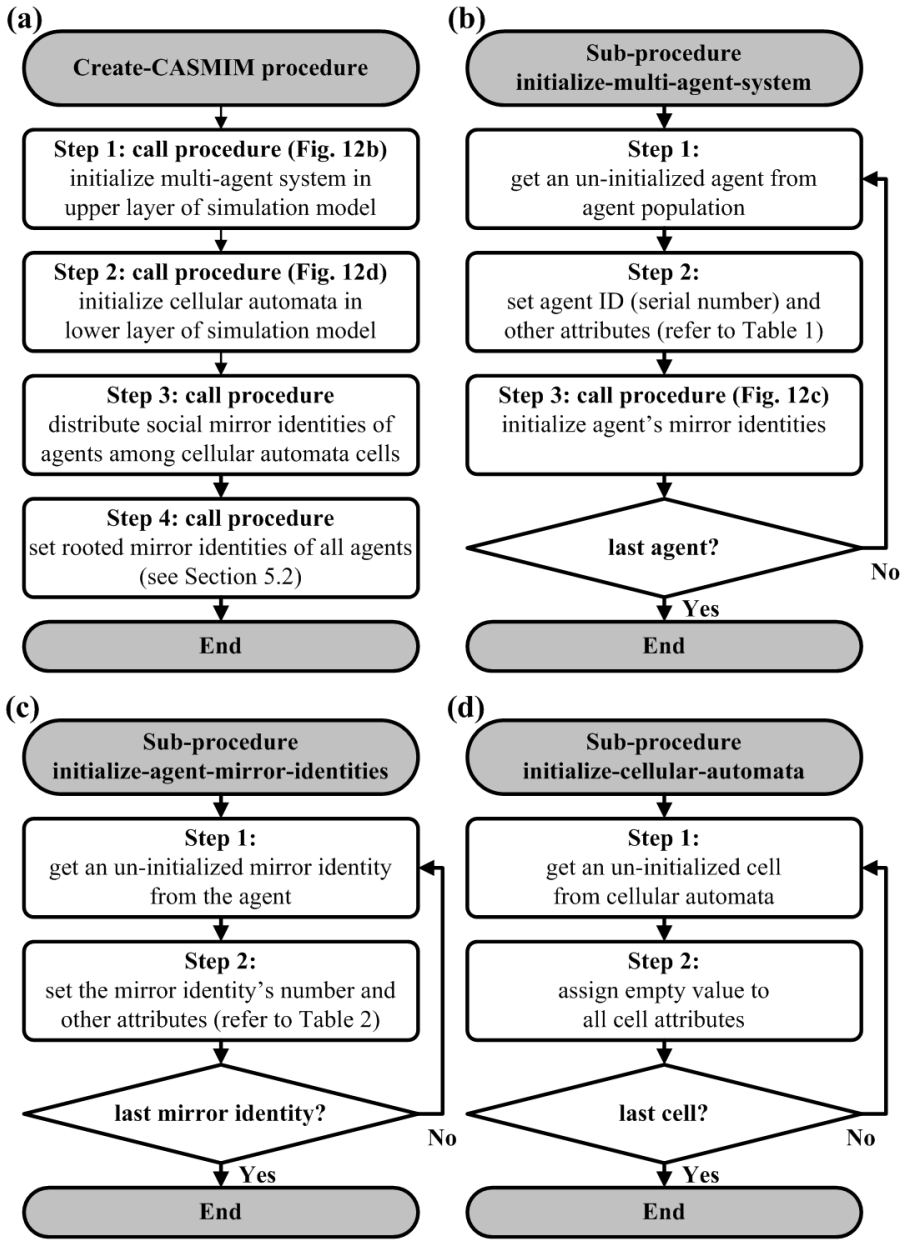

Figure 12. Flowchart for initializing the cellular automata with the social mirror identity model (CASMIM): (a) create-CASMIM procedure, (b) initialize- multiagent-system subprocedure, (c) initialize-agent-mirror-identities subprocedure, and (d) initialize-cellular-automata subprocedure.

the connect-mirror-identity-with-cell subprocedure to perform a two-way reference. At this point, the serial number of the social mirror identity and the ID of the agent that possesses the identity are respectively recorded as the *MirrorIdentityNo* and *AgentID* of the cellular automata lattice. The lattice position is recorded in *Location* (x, y)—the coordinate attribute of the social mirror identity.

3.3 Small-World and Clustering Phenomena in CASMIM

We designed two sensitivity analysis experiments to determine whether our proposed model is (a) a small-world social network with the characteristics of high clustering and low degree of separation and (b) a robust simulation model in which small-world characteristics are not affected

as long as four parameters (cellular automata height, cellular automata width, total agent population, and the upper limit of an agent's mirror identities) are set within reasonable ranges. The first two parameters directly affect the settings of the third and fourth, and vice versa. Corresponding relationships among the four factors are shown in equation (2); the distribute-mirror-identities-to-CA procedure is described in section 3.2.

$$Environment_{CA}.Attribute_H \times Environment_{CA}.Attribute_W = \sum_{A \in Population_{Agent}} |Agent_A.Attribute_{Count}|. \quad (2)$$

Our first experiment focused on the relationship between total agent population and degree of separation. We maintained a fixed average number of agent mirror identities while changing the total agent population, beginning with 2000 and adding 2000 for each simulation up to a total of 200,000. Results are presented in Figure 13; the horizontal axis represents total agent population, and the vertical axis represents average degree of separation for the entire social network. The curves represent four experiments, with the average number of agent mirror identities set at 2, 4, 6, and 8. Each curve shows the average value for 20 runs.

According to our results, an increase in total agent population was accompanied by a slow, logarithmic increase in average degree of separation for the entire social network. The average degree of separation remained sufficiently low to characterize our proposed model as a small-world social network model. In other words, the simulation model will always represent a small-world social network as long as all agents have an average of two or more mirror identities, regardless of total agent population change. The lack of fluctuation in our model's small-world characteristic is an indication of robustness for that parameter, even when the total agent population value changes.

Our second experiment focused on the relationship between average number of agent mirror identities and degree of separation. We maintained a fixed population of 10,000 agents and manipulated the number of agent mirror identities at a rate of 2^n, with n = 0, 1, 2, 3, or 4. In Figure 14, the horizontal axis represents the average number of agent mirror identities, and the vertical axis represents the average degree of separation for the entire social network. The results indicate that when the average number of mirror identities = 1 (i.e., each upper-layer agent has only one mirror identity in the lower-layer cellular automata, which is considered typical of cellular automata), the average degree of separation for the entire social network was very high. When the average number of agent mirror identities increased to 2 or more (with $n \geq 1$), the average degree of separation value decreased to 5.44, indicating the appearance of small-world characteristics. As the average number of agent mirror identities increased to 4 (with n = 2), the curve in Figure 14 slowly decreased and stabilized. In other words, our proposed simulation model resembles a small-world social network as long as the average number of agent mirror identities exceeds 1. Our results indicate that the average number of agent mirror identities is a robust parameter; as long as it remains within a reasonable range ($n \geq 1$), small-world characteristics are not influenced by a change in value.

Figure 15 shows a normalized clustering coefficient curve and the separation coefficient curve (outcome) after normalizing the results of our second experiment. The clustering coefficient $C(Agent)$ can be derived from equation (1), reduced according to the Moore neighborhood parameters and the number of an agent's social mirror identities, and expressed as equation (3) (where $Agent_A.Attribute_{Count}$ represents the number of social mirror identities of agent A). The clustering coefficient $C(Population_{Agent})$ of the entire social network is the average of $C(Agent)$ for all agents.

$$C(Agent) = \frac{3}{8_{\text{ surrounding Moore neighbors}} \times Agent.Attribute_{Count}) - 1}. \quad (3)$$

In Figure 15, the horizontal axis represents the average number of agent mirror identities (increasing by 2^n, with n = 1, 2, 3, and 4), and the vertical axis range of 0 to 1 indicates a normalized unit. The normalized clustering curve consists of small squares, and the average degree of separation curve consists of small triangles. The figure also indicates that when the average number of agent mirror identities = 1, the degrees of separation and clustering are both 1. When the average number of agent mirror identities exceeds 1 and increases gradually, (a) the degree of separation curve rapidly falls to between 0.1 and 0.01, and (b) the clustering curve decreases gradually and maintains a certain distance from the degree of separation curve. However, both curves support the assertion that our proposed model has the small-world social network characteristics of a high degree of clustering and a low degree of separation.

4. Modeling Contagious Epidemics and Setting Parameters

4.1 Modeling Epidemiological Features

When applying our proposed model to examine epidemic transmission dynamics, public health policies, and disease prevention strategies, epidemiologists need to categorize disease statuses according to specific epidemic characteristics, local conditions, and administrative requirements. We applied the state transfer concept of compartmental

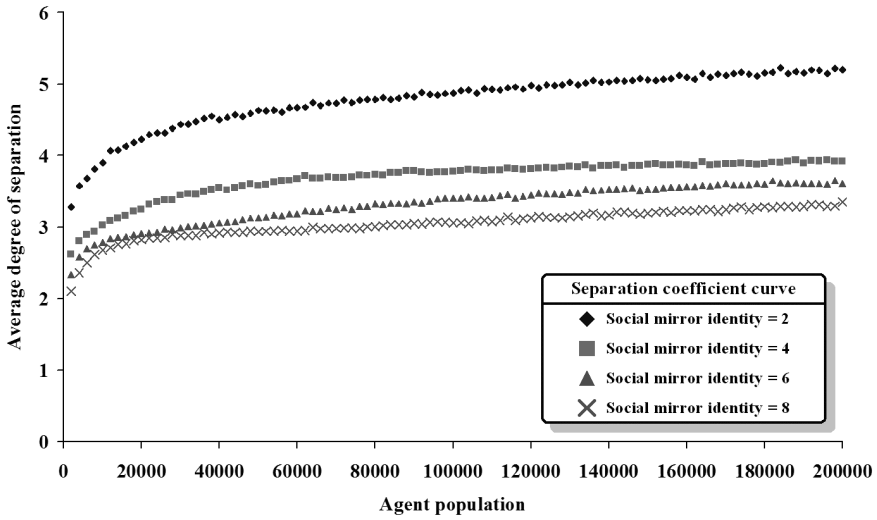

Figure 13. Effect of total agent population on average degree of separation

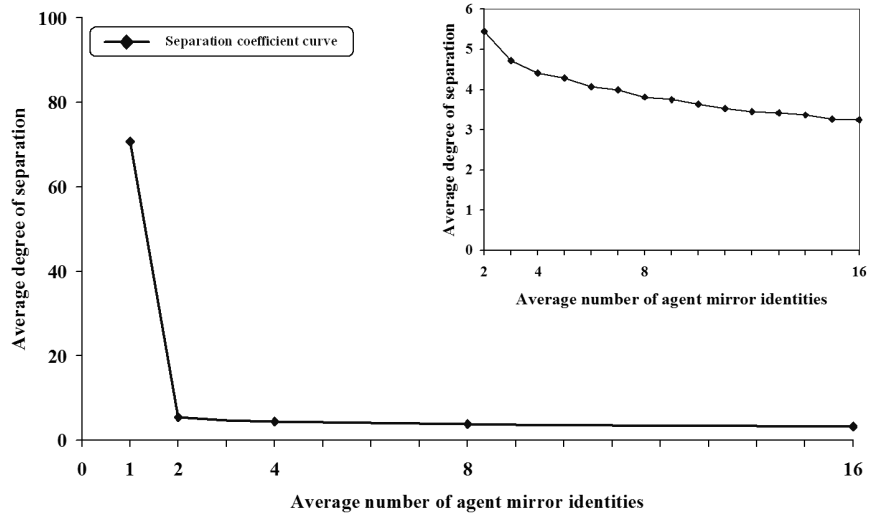

Figure 14. Effect of average number of agent mirror identities on average degree of separation

models and six disease statuses—*S* (Susceptible), *E* (Incubated), *I* (Infectious), *D* (Deceased), *R* (Recovered), and *M* (Immune)—to represent an individual's epidemiological progress state (Fig. 6, Table 1) and the behavioral and transformative results from interactions among individuals.

Before modeling the epidemiological features and public health policies, we assumed that the epidemic was transmitted via close contact and exchanges of saliva. According to the transmission route and social network characteristics used in our simulation, infections were further divided into contact and transmission stages, meaning that an agent's mirror identity had to come into contact with the mirror identity of an adjacent neighbor for an infection to occur.

Based on the combination of $Agent.Attribute.Rate_{Contact}$ and a random number c, each mirror identity of an agent determines whether it will interact individually with the mirror identities of its eight adjacent neighbors. If the value of the *Suspend* attribute for the mirror identity of agent A is false and the random number c is lower than

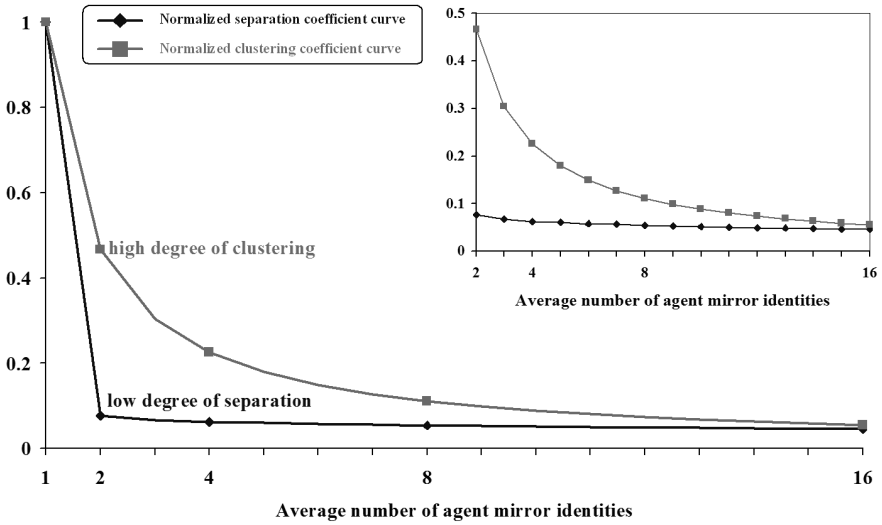

Figure 15. Effect of average number of agent mirror identities on average degree of separation and average clustering coefficient

the contact rate, the mirror identity of agent A comes into contact with the mirror identity of its neighbor agent B. The $Agent.Attribute.Rate_{Contact}$ depends on the enactment of a specific parameter—for instance, "reduced public contact." In this section, we express these concepts using the following pseudo-code:

```
procedure contact is
  for each A ∈ Population_Agent do loop
    for each I ∈ Agent_A.Set_MirrorIdentity
    do loop
     if Agent_A.MirrorIdentity_I.
     Attribute_Suspend = False then
      for each J ∈ Agent_A.Mirror-
      Identity_I.Set_Neighbor do loop
       c ← random(0, 1) // c ∈ [0,1]
       if c ≤ Agent_A.Attribute.Rate_Contact
       then
        infect(Agent_A.MirrorIdentity_I,
        Agent_Trace(J).MirrorIdentity_J)
return

procedure infect (parameter
Agent_A.MirrorIdentity_I,
Agent_B.MirrorIdentity_J) is
  if Agent_A.Attribute_E = I ∧
  Agent_B.Attribute_E = S then
    n ← Random(0, 1) // n ∈ [0,1]
    if n ≤ System.Parameter.Rate_Infection
    then
     comment epidemiological state
     changes from S to E
     Agent_B.Attribute_E ← E // E
     means incubated
     Agent_B.Attribute_Day ← 1
return
```

Assume that agents A and B have adjacent mirror identities; agent A is infected and contagious, and agent B is susceptible and prone to infection. When the two agents come into contact, a combination of infection rate ($System.Parameter.Rate_{Infection}$) and a random number n determines whether or not agent B is infected by agent A. If $n <$ the infection rate, agent B's epidemiological state changes to E (Incubated), and the period attribute ($Agent.Attribute_{Day}$) changes to 1 (denoting that symptoms have not yet appeared and that agent B cannot transmit the disease). The $System.Parameter.Rate_{Infection}$ is determined by such factors as immunity rate—that is, whether agent A is a super-spreader, in home quarantine, in hospital isolation, and so on. Furthermore, agent A's epidemiological state automatically changes from E to I (Infectious) once the incubation period ($System.Parameter.Period_{Incubation}$) is exceeded.

```
procedure handle-epidemiological-
progress-state (parameter Agent_A) is
  ......
  comment epidemiological state changes
  from E to I
  if Agent_A.Attribute_E = E then
    if Agent_A.Attribute_Day > System.
    Parameter.Period_Incubation then
     Agent_A.Attribute_E ← I // I means
     Infectious
```

```
  ......
  comment epidemiological state changes
  from I to R or D
  if Agent_A.Attribute_E = I then
    if Agent_A.Attribute_Day >
    System.Parameter.Period_(Incubation+Infectious)
    then
     d ← random(0, 1) // d ∈ [0,1]
     if d ≤ System.Parameter.Rate_Death
     then
      Agent_A.Attribute_E ← D // D means
      Deceased
      Agent_A.Attribute_Day ← 0
     else
      Agent_A.Attribute_E ← R // R means
      Recovered
      Agent_A.Attribute_Day ← 1
  ......
  comment epidemiological state changes
  from R to M
  if Agent_A.Attribute_E = R then
    if Agent_A.Attribute_Day >
    System.Parameter.Period_Recovered then
     Agent_A.Attribute_E ← M // M means
     Immune
  ......
  comment epidemiological state changes
  from M to S
  if Agent_A.Attribute_E = M∧ not
  Agent_A.Attribute_ImmunityPermanent then
    if Agent_A.Attribute_Day >
    System.Parameter.Period_Immune then
     Agent_A.Attribute_E ← S // S means
     Susceptible
     Agent_A.Attribute_Day ← 0
  ......
return
```

When agent A's epidemiological state is I and it exceeds the $System.Parameter.Period_{Infectious}$ infectious period, a combination of death rate ($System.Parameter.Rate_{Death}$) and a random number d determines whether the agent enters the D (Deceased) or R (Recovered) state. Death rates are influenced by such factors as age, whether or not the agent was placed under home quarantine during its incubation and infective periods, whether it received treatment in hospital isolation, and its public activities during the illness period.

When agent A's epidemiological state is R and it exceeds the $System.Parameter.Period_{Recovered}$ recovery period, it automatically enters an M (Immune) state. In this state, the $Agent.Attribute_{ImmunityPermanent}$ parameter determines whether agent A's immunity is permanent or temporary—that is, whether complete recovery or renewed susceptibility occurs following $System.Parameter.Period_{Immune}$.

4.2 Modeling Social Mobility, Families, and Hospitals

Mirror identities have two private attributes: *Root* and *Suspend* (Table 2). As shown in the following pseudo-codes (for the set-rooted-mirror-identities-of-all-agents procedure), the *Root* attribute for most agents is true for one mirror identity but false for all others. In contrast, the *Suspend* attribute is false for all of an agent's mirror identities. To facilitate our discussion, we will assume the presence of a rooted mirror identity—that is, one whose *Root* attribute is always true. Rooted mirror identities can be used to represent one-of-a-kind units such as homes, dormitories, and hospitals.

```
procedure set-rooted-mirror-identities-
of-all-agents is
  for each A ∈ Population_Agent do loop
    for each I ∈ Agent_A.Set_MirrorIdentity
    do loop
     Agent_A.MirrorIdentity_I.
     Attribute_Suspend ← False
     Agent_A.MirrorIdentity_I.
     Attribute_Root ← False
    n ← random(1, Agent_A.Attribute_Count)
    // n ∈ [1,Agent_A.Attribute_Count]
    Agent_A.MirrorIdentity_Index(n).
    Attribute_Root ← True
    Agent_A.Attribute_Mobility ← Free
return
```

If a health authority puts agent A under home quarantine (i.e., the mobility attribute of agent A is changed to *Quarantined*), the *Suspend* attributes of all its mirror identities are marked as true with the exception of its rooted mirror identity. Accordingly, agent A cannot interact with other adjacent neighbors or move among various locations with the exception if it is home until the quarantine period ends. The lattice points surrounding agent A's rooted social mirror identity are the mirror identities of the agent's family members and/or cohabitants. Once the home quarantine is lifted, the *Suspend* attributes of all mirror identities except for the rooted mirror identity return to false, indicating a resumption of normal activities.

```
when event Agent_A.Attribute_Mobility
= Quarantined do
    for each I ∈ Agent_A.Set_MirrorIdentity
    do loop
     if Agent_A.MirrorIdentity_I.
     Attribute_Root = False then
      Agent_A.MirrorIdentity_I.
      Attribute_Suspend ← True

when event Agent_A.Attribute_Mobility
 = Free do
  for each I ∈ Agent_A.Set_MirrorIdentity
   do loop
    Agent_A.MirrorIdentity_I.
    Attribute_Suspend ← False
```

The advantage of our proposed model is that it does not require fixed lattice points for representing hospitals. Assume that agent B, with a confirmed epidemiological state of I, voluntarily enters isolation (i.e., its mobility attribute changes to *Isolated*). Similar to the preceding example, the *Suspend* attributes of all agent B mirror identities (except for its rooted mirror identity) are changed to true. This represents a scenario where agent B is receiving treatment in hospital isolation. The lattice points surrounding agent B's rooted mirror identity represent medical staff, nurses, health care workers, and perhaps one or more family members who have special visitation privileges. If agent B recovers, the *Suspend* attributes of the affected mirror identities return to false, indicating a resumption of normal activities. If the agent dies, the *Suspend* attributes of agent B's mirror identities (including its rooted mirror identity) are permanently changed to true.

```
when event Agent_A.Attribute_Mobility
= Isolated do
  for each I ∈ Agent_A.Set_MirrorIdentity
  do loop
    if Agent_A.MirrorIdentity_I.
    Attribute_Root = False then
     Agent_A.MirrorIdentity_I.
     Attribute_Suspend ← True

when event Agent_A.Attribute_Mobility
= Free ∧ Agent_A.Attribute_E = R do
  for each  I ∈ Agent_A.Set_MirrorIdentity
  do loop
    Agent_A.MirrorIdentity_I.
    Attribute_Suspend ← False

  when event Agent_A.Attribute_Mobility
   = Free ∧ Agent_A.Attribute_E = Ddo
  for each I ∈ Agent_A.Set_MirrorIdentity
  do loop
    Agent_A.MirrorIdentity_I.
    Attribute_Suspend ← True
```

Table 5 presents the results of an intersection between epidemiological progress states and mobility states. The table allows users to address various potential combinations of situations that can occur during an epidemic outbreak. Health authorities can use this information to test various public health policies—for instance, decreasing or completely eliminating the number of infectious patients who are allowed to leave their homes or hospitals (i.e., individuals with a disease status of E or I and a social activity status of *Free*, or with a disease status of S and a social activity status of *Quarantined* or *Isolated*).

4.3 Modeling Public Health Policies

4.3.1 Mask-Wearing Policy: General Public vs. Health Care Workers

The two parameters for a general public mask-wearing policy are participation rate (the percentage of individuals in the total population who actually wear masks) and prevention efficiency (the protection grade of the masks being used). Our simulation system uses the participation rate to select agents who abide by the policy. Agents with an S-status who wear masks are much less likely to become infected, depending on the prevention efficiency parameter. The same is true for I-status agents who wear masks before and after their symptoms appear since the probability of the disease being spread to its neighbors will decrease, also depending on the prevention efficiency parameter.

The process for simulating a hospital employee mask-wearing policy is essentially the same. Once the policy is put into effect, agents who surround the rooted mirror identities of agents in hospital isolation either wear or do not wear masks based on the participation rate, and the probability of infection is also affected by the prevention efficiency parameter. Due to the high potential for infection, health care workers are usually required or strongly encouraged to wear masks with high protection rates, making their participation rates very high. Since they tend to wear better quality masks, the prevention efficiency is also high.

```
when a mask-wearing policy in general
public is enacted or changed do
  if Policy_WearningMaskInGP.Parameter.
  Rate_Participation > 0 then
    for each A ∈ Population_Agent do loop
     n ← random(0, 1) // n ∈ [0,1]
     if n ≤ Policy_WearingMaskInGP.Parameter.
     Rate_Participation then
      Agent_A.Attribute_WearingMask ← True
      Agent_A.Attribute_MaskType ←
      Policy_WearingMaskInGP.Parameter.
      Rate_Prevention
     else
      Agent_A.Attribute_WearingMask ← False

when a mask-wearing policy in health
worker is enacted or changed do
  when event Agent_A.Attribute_Mobility
   = Isolated do
    for each N ∈ Agent_A.Mirror-
    Identity_Root.
    Set_Neighbor do loop
     c ← random(0, 1) // c ∈ [0,1]
     if c ≤ Policy_WearningMaskInHW.Parameter.
     Rate_Participation then
      Agent_Trace(N).Attribute_WearingMask ←
      True
      Agent_Trace(N).Attribute_MaskType ←
      Policy_WearingMaskInHW.Parameter.
      Rate_Prevention
     else
      Agent_Trace(N).Attribute_WearingMask ←
      False
```

Table 5. Intersection between epidemiological progress and social mobility states

Epidemiological Progress State	Mobility State	Description
Susceptible	*Free*	Agent is healthy and free to move anywhere.
Susceptible	*Quarantined*	Agent is healthy but in quarantine since it may come into contact with an infectious agent.
Susceptible	*Isolated*	Agent is healthy but is mistakenly diagnosed as infected and therefore isolated by health care center.
Incubated	*Free*	Agent is infected and in an incubation period. It is free to move anywhere because it has not been properly diagnosed.
Incubated	*Quarantined*	Agent is infected and in an incubation period. It has yet to be examined. There is a possibility that one of its friends or family members has been diagnosed as infected; therefore, the agent is quarantined according to contact tracing and home quarantine policies.
Incubated	*Isolated*	Agent is infected and in an incubation period. After being examined, it is placed in hospital isolation.
Infectious	*Free*	Agent is infected and has symptoms, but it has yet to be examined or affected by a contact tracing policy. It can move anywhere and can easily infect other agents.
Infectious	*Quarantined*	Agent is infected and has symptoms, but it has yet to be examined. There is a possibility that one of its friends or family members has been diagnosed as infected; therefore, the agent is quarantined according to contact tracing and home quarantine policies.
Infectious	*Isolated*	Agent is infected and has symptoms. After being examined and diagnosed, it is placed in hospital isolation.
Deceased	*None*	Agent is dead.
Recovered	*Free*	Agent is recovered and free to move anywhere.
Recovered	*Quarantined*	Agent is recovered but is kept in quarantine because it has been in close contact with someone who has been diagnosed with the disease.
Recovered	*Isolated*	Agent is recovered but still in hospital isolation.
Immune	*Free*	Agent is immune and can move anywhere.

4.3.2 Taking Body Temperature

Under a temperature measurement policy, the social mirror identities of individual agents decide individually whether or not to measure their body temperatures before coming into contact with their surrounding social mirror identities. Their decisions are made based on a combination of a participation rate parameter and a random number n. An n that is lower than the participation rate means that neighboring agents are following the practice of measuring the temperatures of all agents that want to contact them. Success thereby depends on the detection rate parameter—a combination of participation rate and thermometer accuracy. During the 2003 SARS epidemic, most countries accepted the World Health Organization (WHO) recommendation to enforce this policy, but execution was considered expensive in terms of manpower and social costs. It was relatively easy for infected individuals to avoid having their body temperatures taken.

4.3.3 Reducing Public Contact

Some researchers have recently studied reduced public contact as a means of controlling the spread of disease [7, 10]. In our simulation, the infection process was affected by a combination of contact and infection rate. Reducing public contact decreased the contact frequency of a targeted group of agents. The combination of participation rate and a random number n determined whether the mirror identities of two agents interacted. An n that exceeded the participation rate indicated that an agent avoided contact with the mirror identities of its neighboring agent.

4.3.4 A- and B-Class Home Quarantines

According to an A-class home quarantine policy, whenever an infected agent is identified, all agents surrounding the infected agent's mirror identities must decide whether they accept home quarantine, based on the participation rate parameter. If they do, their mobility attribute changes from *Free* to *Quarantined*. As in the hospital isolation example, all of the mirror identities of agents that decide to enter home quarantine become inactive until the separation period is complete. This requirement does not apply to rooted mirror identities. This policy requires considerable manpower and social costs to execute.

Although similar in most respects to the A-class policy, a B-class policy affects a larger number of agents. For instance, if one mirror identity of agent C is adjacent to a particular mirror identity of agent D (i.e., if agents C and D are a cohabiting couple), this represents one degree of separation. If one mirror identity of agent D is adjacent to a particular mirror identity of agent E (perhaps coworkers in the same office), this represents two degrees of separation between agents E and C. Under a B-class policy, both D and E would be required to enter home quarantine.

4.3.5 Hospital Access

During the 2002-2003 SARS epidemic, Singaporean and Taiwanese health authorities imposed strict rules concerning hospital visitations [10]. To simulate this "hospital access control" policy, we assumed that agent A showed symptoms and was admitted to a hospital for treatment in isolation. If the rooted mirror identities of agents A and B are adjacent, this indicates that agent B is on the hospital staff, a nurse, a health care worker, or a very close relative. If agent C's nonrooted mirror identities are adjacent to agent A's rooted mirror identity, it indicates that agent C is a distant relative, friend, classmate, or coworker. Under a strict visitation policy, agent B is allowed to come into contact with agent A, but agent C is not.

4.4 Basic Reproductive Number R_0 with Corresponding Parameters in CASMIM

To present a reasonable and precise picture of the transmission dynamics of an epidemic, we adjusted certain parameters according to the most recently available information on contact rate, transmission rate, number of contacts, and average transmission period. In addition to predicting and estimating overall disease trends, we also applied the basic case reproduction number R_0 to estimate all values for the parameters just described to increase the precision and reliability of the simulation process and outcome.

According to Anderson and May [27] and Becker [28], R_0 can be expressed as equation (4), where c represents the number of times an infectious person comes into contact with an uninfected person, β is the probability of transmitting the infection to each contact, and D is the length of time a person remains infectious.

$$R_0 = c \times \beta \times D. \tag{4}$$

According to the characteristics of our proposed model, equation (4) can be amended as equation (5). β and D are the same in both equations, with β replacing the infection rate $R_{Infection}$ ($System.Parameter.Rate_{Infection}$) and D replacing the average infected period $P_{infectious}$ ($System.Parameter.Period_{Infectious}$).

$$R_0 = (\text{avg. of social mirror identity} \times \text{no. of neighbors} \times R_{Contact} \times T_{Contact}) \times R_{Infection} \times P_{Infectious}. \tag{5}$$

As shown in equation (5), element c in equation (4) can be broken down, with "avg. of social mirror identity" representing the average number of agent mirror identities, "no. of neighbors" the number of neighbors for each mirror identity (which under the Moore neighborhood structure equals 8), $R_{Contact}$ ($Agent.Attribute.Rate_{Contact}$) the contact rate of an agent's mirror identity and the mirror identities of its neighbors, and $T_{Contact}$ ($System.Parameter.Frequency_{Contact}$) the average number of contacts of an agent's mirror identity with the mirror identities of any other neighbor during a time step.

Since the average numbers of mirror identities for an agent and its neighbors are constants, they do not require updating, even when other disease transmission parameters change. Thus, only four parameters in equation (5) are associated with epidemics: contact rate ($R_{Contact}$), number of contacts ($T_{Contact}$), transmission rate ($R_{Infection}$), and average infected period ($P_{Infectious}$). All of these require adjustment according to the latest information released by health authorities.

5. Simulating SARS with CASMIM

5.1 Comparing Simulation Results with Actual Cases

After initializing our model and setting up system and epidemic disease parameters (Table 3) according to information distributed by WHO and the U.S. Centers for Disease Control and Prevention (CDC) [7, 10, 41-48], we simulated the transmission dynamics of SARS in different areas and compared the effectiveness of various public health policies and disease prevention strategies. We used the simulation definitions and parameters identified in section 4 and assumed that one time step = 1 day in the real world.

Since SARS originated in China's Guangdong province, we viewed the SARS viruses in all other countries as being imported and used the number of imported cases announced by local health authorities to determine transmission source information—for example, number of infectious people entering a country, the time step during which they entered, and whether they entered as incubated or infected individuals (Tables 6-9). We incorporated public health policies at certain time steps according to actual announcements made by local health authorities and adjusted our simulation environment, epidemic, and public health policy parameters according to data from the CDC [42, 44, 45, 47] and Sebastian and Hoffmann [10].

5.1.1 Statistical Analyses for Epidemic Simulation

We used five statistical tests to examine the reliability and validity of time-series data generated by the simulation system (Table 10): a chi-square test for homogeneity of proportions, a correlation coefficient (CC, equation (6)), coefficient of efficiency (CE, equation (7)), mean square error (MSE, equation (8)), and mean absolute error (MAE, equation (9)). $\{X_t | \ t = 1 \ldots n \wedge t \in \aleph\}$ represents time-series data for the number of individuals who were actually infected each day. $\{Y_t | t = 1 \ldots n \wedge t \in \aleph\}$ represents time-series data for the numbers of infected individuals each day generated by our simulation system. In both data sets, t represents the time step (ranging from 1 to a maximum value of n), X_t represents the number of actual infected individuals at time step t, Y_t represents the number of infected individuals generated by the simulation system at time step t, $\overline{X}$ represents the mean number of actual infected individuals, and $\overline{Y}$ represents the mean number of infected individuals in the simulation.

Table 6. Input data for simulating SARS epidemic curves in Taiwan, Singapore, and Toronto

Category	Attribute	Data Type	Description	Default Value
Imported Cases	*Time Point*	Date	Date when imported case occurred.	
	Amount	Integer	Number of patients.	
	Phase	Symbol	Imported during incubation or illness period.	Infected
	Super-spreader	Boolean	Determine whether the imported patient is a super-spreader.	False
Public Health Policy	*Related Attributes*	See Table 4		
Run	*Day*	Integer	Number of execution days.	

Table 7. Singapore simulation input data

Time Step	Action	Persons	State	Public Health Policy	Special Description on the Simulator
2003/3/1	Trigger	1	Infectious		Super-spreader
2	Trigger	2	Infectious		
11	Set			Reduced public contact	Efficacy = 0.9, Participation = 0.5
15	Trigger	1	Incubation	Mask-wearing policy for health care workers	Efficacy = 0.9, Participation = 0.9
22	Trigger	2	Incubation		
				Home quarantine	10 days, Participation = 0.9
23	Set			Controlling hospital access	Efficacy = 0.9, Participation = 0.9
				Mask-wearing policy for general public	Efficacy = 0.9, Participation = 0.5
25	Trigger	2	Infectious		
52	Set			Taking body temperature	Efficacy = 0.9, Participation = 0.5

Table 8. Taipei simulation input data

Time Step	Action	Persons	State	Public Health Policy	Special Description on the Simulator
2003/3/20	Trigger	1	Infectious		
2	Trigger	4	Incubation		
9	Trigger	1	Incubation		
11	Trigger	2	Infectious		
12	Trigger	2	Infectious	Home quarantine	10 days, Participation = 0.9
14	Trigger	1	Infectious		
27	Trigger	1	Infectious	Mask-wearing policy for health care workers	Efficacy = 0.9, Participation = 0.9
47	Set			Controlling hospital access	Efficacy = 0.9, Participation = 0.9
53	Set			Home quarantine	14 days, Participation = 0.9
				Mask-wearing policy for general public	Efficacy = 0.9, Participation = 0.5
74	Set			Home quarantine	10 days, Participation = 0.9
88	Set			Taking body temperature	Efficacy = 0.9, Participation = 0.5

$$CC = \frac{\sum_{t=1}^{n}\left(X_t - \overline{X}\right) \times \left(Y_t - \overline{Y}\right)}{\sqrt{\sum_{t=1}^{n}\left(X_t - \overline{X}\right)^2 \times \sum_{t=1}^{n}\left(Y_t - \overline{Y}\right)^2}} \in [-1, 1], \tag{6}$$

$$CE = 1 - \left[\frac{\sum_{t=1}^{n}(X_t - Y_t)^2}{\sum_{t=1}^{n}\left(X_t - \overline{X}\right)^2}\right] \in [0, 1], \tag{7}$$

$$MSE = \frac{1}{n}\sum_{t=1}^{n}(Y_t - X_t)^2 \in [0, \infty], \tag{8}$$

$$MAE = \frac{1}{n}\sum_{t=1}^{n}|(Y_t - X_t)| \in [0, \infty]. \tag{9}$$

With the exception of the chi-square test, none of the statistical tests requires a table lookup to evaluate simulation

Table 9. Toronto simulation input data

Time Step	Action	Persons	State	Public Health Policy	Special Description on the Simulator
2003/2/23	Trigger	1	Infectious		
6	Trigger	1	Infectious		
19	Trigger	1	Infectious	Mask-wearing policy for health care workers	Efficacy = 0.9, Participation = 0.9
				Reduced public contact	Efficacy = 0.9, Participation = 0.5
30	Trigger	1	Infectious		
				Controlling hospital access	Efficacy = 0.9, Participation = 0.9
37	Set			Home quarantine	10 days, Participation = 0.9
38	Trigger	1	Infectious		
68	Close			All public health policies previously opened	
91	Set			Mask-wearing policy for health care workers	Efficacy = 0.9, Participation = 0.9
112	Set			All public health policies previously closed	

Table 10. Reliability and validity tests for epidemic simulation using CASMIM

	Reliability Test				Validity Test			
	Chi-Square Test for Homogeneity of Proportions							
Simulated Area	Degree of Freedom	χ^2	$\chi^2_{0.05,\text{ degree of freedom}}$	P	CC	CE	MSE	MAE
Singapore	70	55.54	90.53	0.896	0.6943	0.9926	6.31	1.75
Taipei	87	100.48	109.77	0.153	0.7698	0.9948	15.00	2.36
Toronto	111	107.39	136.59	0.500	0.4201	0.9923	4.96	1.69

Note: CC = correlation coefficient; CE = coefficient of efficiency; MSE = mean square error; MAE = mean absolute error.

reliability or validity; in other words, the statistical estimates can be directly applied for evaluation. The closer the CC approaches 1, the higher the positive correlation between the actual and simulation data; the closer to –1, the more likely a negative correlation will result; and the closer to 0, the lower the chances of any correlation between the two. The estimated value of the CE is a real number between 0 and 1. The closer it approaches 1, the higher the accuracy of the simulation. Both MSE and MAE use real numbers between 0 and infinity to represent degree of inaccuracy. The closer it approaches 0, the more accurate the simulation.

We adopted a chi-square test for homogeneity of proportions and a correlation coefficient (CC) to examine the actual number of daily SARS-infected individuals in each city and the numbers that were generated by the simulation system in order to determine whether the distribution proportions for the two sets of time-series data were consistent and reflected a positive correlation. According to the results shown in Table 10, the chi-square test values χ^2 for each city were smaller than $\chi^2_{(0.05,\text{ degree of freedom})}$. We therefore accepted the null hypothesis that the distribution proportions for the time-series data for the number of actual and simulated affected individuals in each city were consistent at a $\alpha = 0.05$ level of significance. After examining the simulation time-series data for the three cities, we found three positive correlations with the actual time-series data.

In terms of simulation validity, if we only examined simulation accuracy according to the MSE and MAE, the respective accuracy data for Toronto (4.96 and 1.69) were higher than for Singapore (6.31 and 1.75) and Taipei (15.00 and 2.36). However, when the CE was applied, the results were the opposite: the value for Taipei (0.9948) was higher than for Singapore (0.9926) or Toronto (0.9923). The reason for this is that the efficiency coefficient primarily considers variables, while MSE and MAE focus on average total error values.

5.1.2 Singapore SARS Outbreak

A comparison of actual and simulated SARS cases in Singapore (Fig. 16) shows that our simulated curve had a very close fit with data published by the city-state's health authority for the two outbreaks that occurred between February 25 and May 5, 2003 (Table 7) [7, 10, 42, 46, 48]. Emergency public health policies were not activated

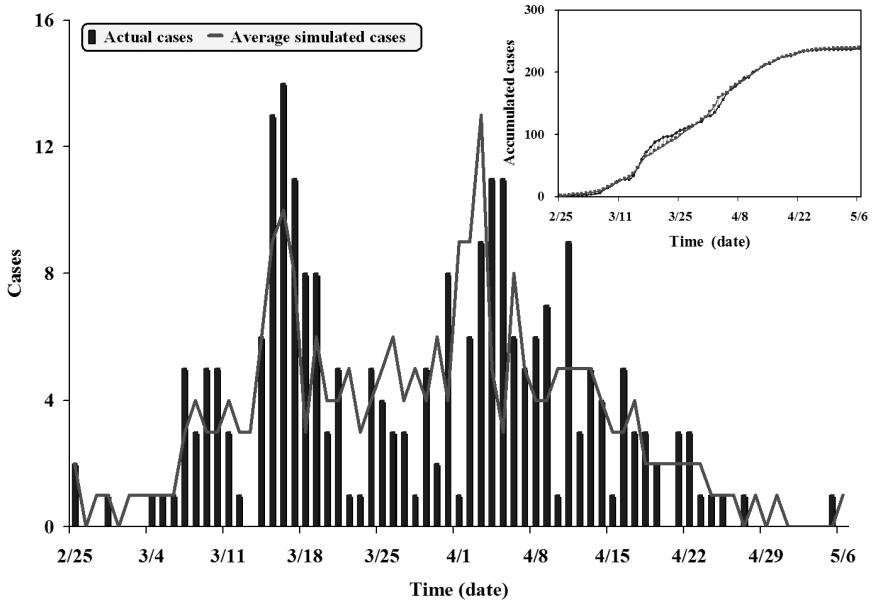

Figure 16. A comparison of actual and simulated epidemic results for the SARS outbreak in Singapore. Blue bars represent actual reported cases; red line represents an average of results from 20 simulation runs.

following the first outbreak, which was attributed to imported cases. The second outbreak was attributed to the compound effects of secondary infections. Several emergency policies were put into effect on March 24, including a ban on visits to patients in hospitals or under home quarantine. The number of new cases dropped dramatically at the beginning of June; soon afterwards, WHO announced that the disease was under control.

5.1.3 Taipei SARS Outbreak

Our Taipei simulation included several public health policies enforced by that city's government, including several grades of home quarantine and a mask-wearing requirement for all bus and train passengers (Table 8) [7, 10, 44, 46-48]. As shown in Figure 17, our simulated results had a close fit with the probable cases curve published by the Taiwanese health authority on September 28, 2003—a major spike followed by several smaller outbreaks. The higher concentration in the Taipei curve compared to Singapore's is likely due to late case discoveries, delays in seeking treatment, illness cover-ups, public interactions, and the large number of cases imported by travelers returning from Hong Kong. In Singapore, all imported cases were reported prior to the first outbreak, and the second wave resulted from compound infections. The S-curve for the Taiwan situation is more representative of a typical infection pattern.

5.1.4 Toronto SARS Outbreak

The SARS scenario in Toronto consisted of two major waves with almost no new cases in between (Fig. 18) [7, 10, 43, 45-46, 48]. However, after a reexamination of the data in August 2003, the Canadian authorities acknowledged several additional cases during the lull period. According to our simulation, the second wave would not have been as severe if strict public health policies had been enforced for a longer period following the first wave. In our simulation (Table 9), we relaxed epidemic control measures (especially restricted hospital access and reduced public contact with infected persons) after the first wave subsided. As a result, a second spike occurred in our simulation within a few days of the actual spike reported by the Toronto health authorities. Our results support Sebastian and Hoffmann's [10] conclusion that the Toronto government lifted its control measures too quickly. Because of increased contact between patients and visitors and relaxed rules on wearing masks and/or respirators by health care workers, Toronto experienced a second nosocomial transmission period.

5.1.5 Home Quarantines

After releasing data on the global SARS outbreak on March 12, 2003, WHO officials recommended that home quarantine periods be at least twice as long as the then-average 4- to 6-day incubation period [7, 10, 42, 47]. The governments of Singapore, Taiwan, and Canada accepted this recommendation and enforced 10-day quarantine policies for the duration of the epidemic; for a short period, the Taiwanese government enforced a 14-day policy. We used the home quarantine policy to test our model and observed that a minimum 10-day quarantine period was required to suppress the number of new cases—the same time period

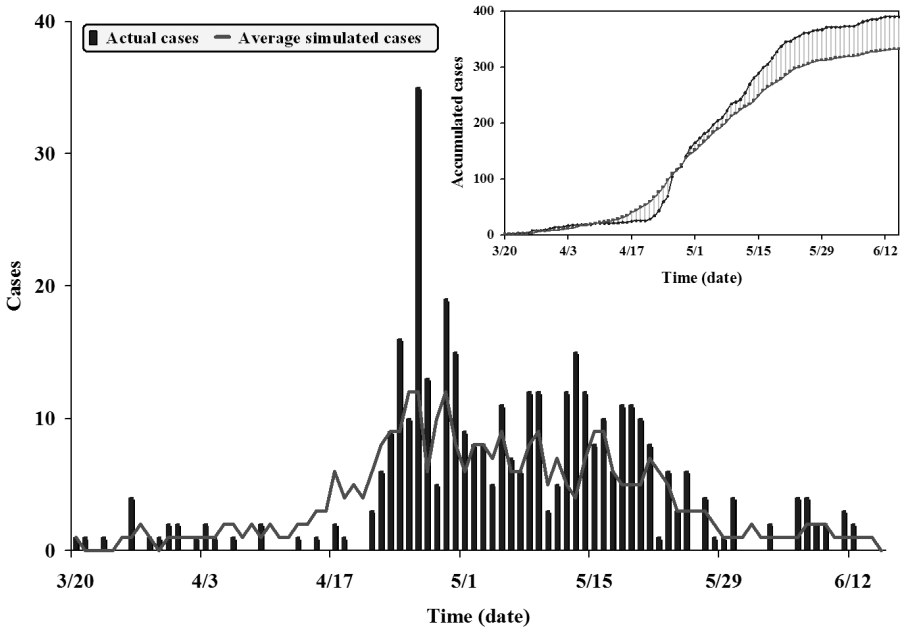

Figure 17. A comparison of actual and simulated epidemic results for the SARS outbreak in Taipei

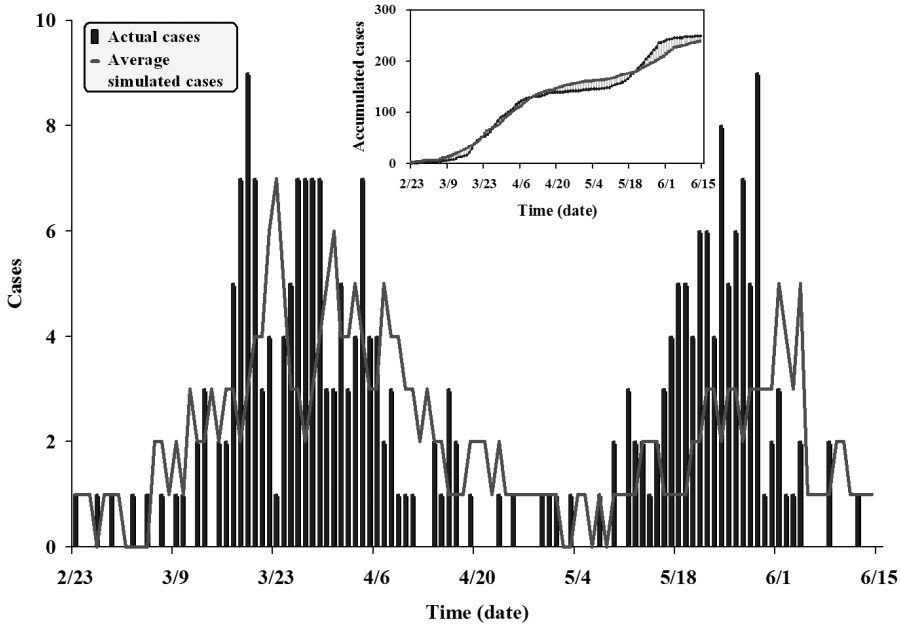

Figure 18. A comparison of actual and simulated epidemic results for the SARS outbreak in Toronto. We assumed that the second outbreak occurred because preventive policies were relaxed too soon following the first outbreak.

recommended by WHO (Fig. 19). Our simulation showed that the disease became endemic when the 10-day quarantine policy was enforced.

5.2 Analyzing Public Health Policies

5.2.1 Taking Body Temperature

The Singaporean and Taiwanese governments both implemented temperature measurement policies during the epidemic, going so far as to launch national campaigns that included installing temperature-monitoring equipment and setting up manual temperature measurement stations at various government buildings, clinics, and public transportation facilities [7, 10]. According to our simulation results, when such policies were both comprehensive and compulsory, they reduced the number of feverish individuals entering public places. However, in the real world, this policy is difficult to set up and enforce since implementation methods tend to vary, oversights are common, and an unknown number of individuals manage to evade having their temperatures taken.

Our simulation results suggest that a participation rate of between 80% and 90% is required for this public health policy to have a positive effect in controlling a SARS epidemic (Fig. 20). At a rate of 65% or lower, it had little effect. This policy incurs significant social costs—for instance, distributing inexpensive thermometers, setting up temperature screening stations, and employing workers to take manual temperature measurements at various public facilities and medical clinics.

5.2.2 Wearing Masks with Different Protection Levels—General Public vs. Health Care Workers

The efforts of the governments of Taiwan and Hong Kong to promote general mask-wearing policies led to hoarding and panic buying [7, 10]. Masks are categorized according to grade—ordinary, surgical, N95 respirator masks, and so on. In Taiwan, a serious shortage of professional masks for medical staff occurred following a mad rush by the general population to purchase masks regardless of grade; this triggered a debate on the necessity of wearing N95 respirator masks outside of hospitals and clinics.

According to the results of a simulation that we ran to analyze this policy, ordinary and surgical masks assisted in controlling the epidemic outbreak as long as wearing them was a strong habit for the desired time period (Fig. 21). At a prevention efficiency of 65% or more (i.e., the mask covered the mouth and nose), the epidemic could be controlled but not eliminated. When wearing ordinary masks, medical staff members still had relatively high infection rates (Figs. 21 and 22); these personnel clearly benefited from wearing N95 and other high-resistance masks in hospitals and other medical centers. From our simulation, we suggest that the general public should not be required to wear high-resistance masks and that higher grade masks should be reserved for medical staff and health care workers.

5.3 Assessing Public Health Suites

Different public health policies entail different social costs. Home quarantining is very effective but requires considerable amounts of labor and material resources compared to temperature measurement and mask-wearing policies. We ran simulations of various prevention strategies to identify an optimal combination of public health policies in terms of efficacy and cost. According to our results, a combination of mask wearing by the general public and reduced contact in public places was the best combination for suppressing the spread of SARS (Fig. 23). Some costs are involved in purchasing masks, but few costs are associated with limited public contact. In addition, mask wearing addresses an epidemic at its source—disease transmission.

The combination of temperature measurement, restricted hospital visitations, and mask wearing by health care workers should be considered a remedial reaction to a SARS outbreak since it is ineffective in terms of preventing patients in the incubation stage or patients suffering from minor symptoms from spreading the disease to others. In addition, this suite requires substantial amounts of labor and material resources. Furthermore, the combination of home quarantine and reduced contact in public places also has high social costs, with results dependent on how well isolation guidelines are followed. Numerous instances of intrafamily infections were reported during the actual 2002-2003 SARS outbreak—evidence that certain prevention strategies were ineffective in controlling the epidemic.

6. Conclusion

In this article, we proposed a novel small-world model consisting of cellular automata with social mirror identities representing daily-contact social networks for running epidemiological simulations. We established the social mirror identity concept to integrate long-distance movement and geographic mobility into the model, which can be used to simulate the transmission dynamics of infectious diseases among social networks and to investigate the efficacies of various public health policies and epidemic prevention strategies—alone and in combination. The model successfully exhibits epidemiological behaviors in the form of daily interactions among heterogeneous individuals and expresses such present-day small-world properties as high degrees of clustering, low degrees of separation, and long-distance movement.

According to the results of simulations that we ran based on data collected during the 2002-2003 SARS outbreaks in Singapore, Taipei, and Toronto, we suggest that this model can be applied to different infection scenarios and used to simulate the development of epidemics with considerable accuracy. A comparison of simulation and real-world data indicates that our model can be used to test epidemic report systems and to identify the best public health policy suites for specific scenarios. The simulation results also indicate

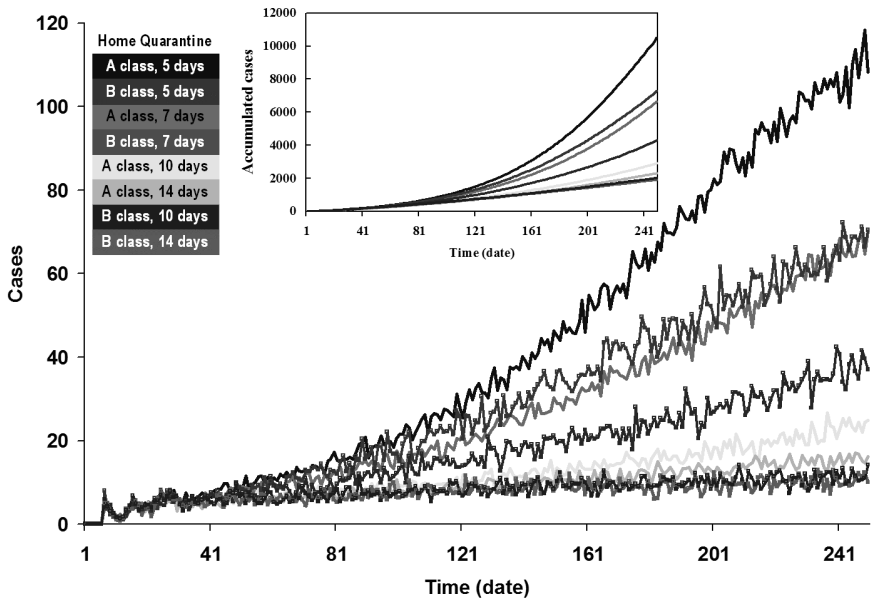

Figure 19. Results from a simulation based on various home quarantine policies. Simulation period was 250 days, with a 5-day default incubation period. According to the results, (a) different home quarantine restriction levels exerted different impacts on the SARS epidemic, and (b) a home quarantine policy by itself was insufficient for suppressing the epidemic.

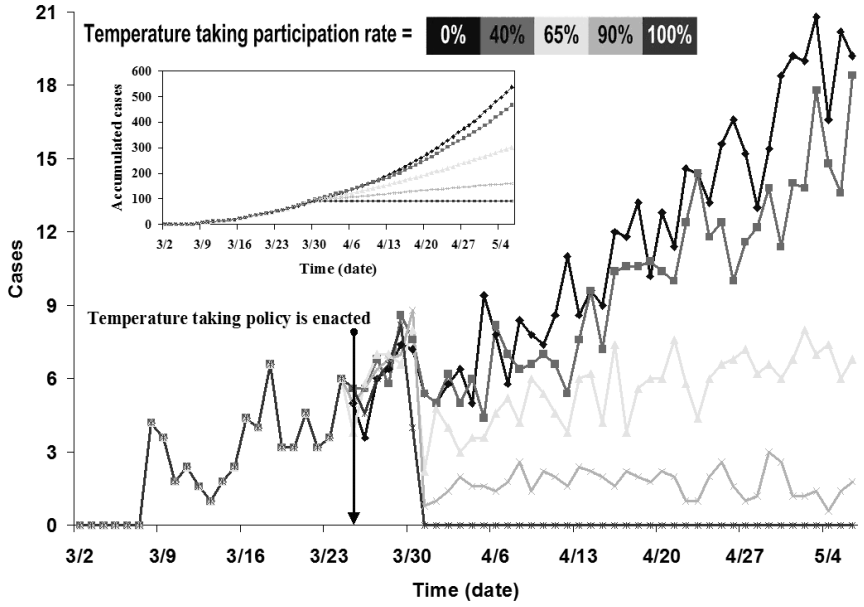

Figure 20. Results from a simulation focused on temperature measurement policy at different participation levels. We used the eight imported cases reported in Singapore to trigger the simulation. In each 66-day simulation run, the policy was activated on day 24.

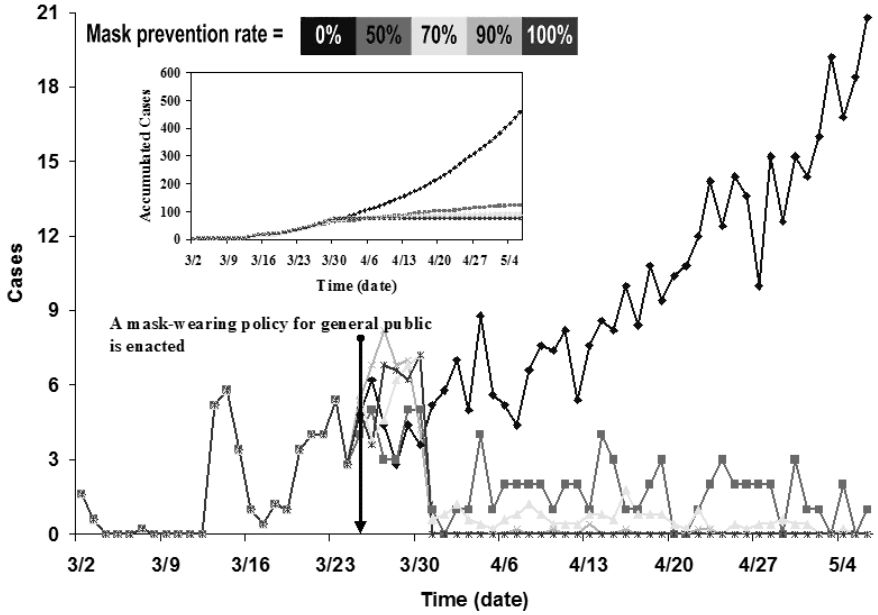

Figure 21. Results from a simulation focused on the impact of mask wearing by the general public, comparing different mask protection levels

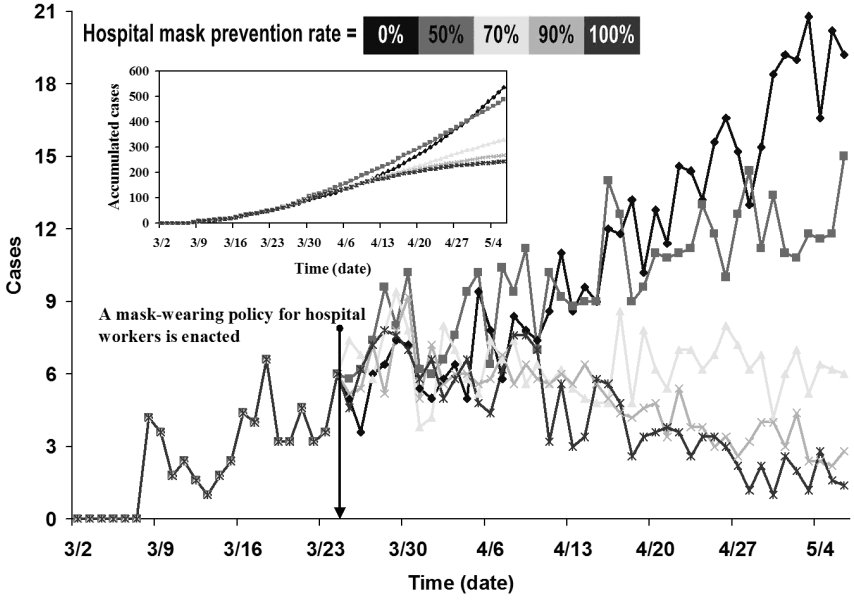

Figure 22. Results from a simulation focused on the impact of mask wearing by health care workers in health care facilities, comparing different mask protection levels

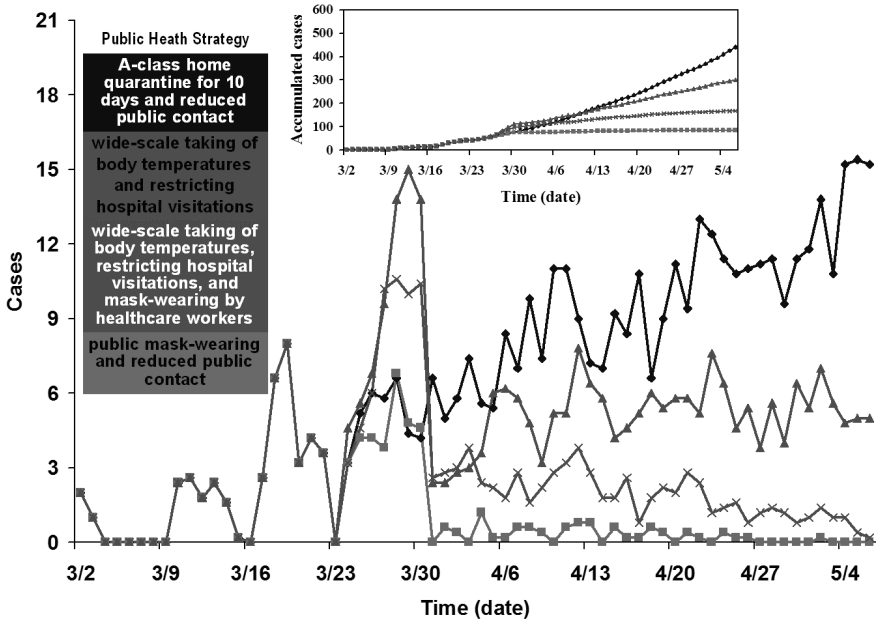

Figure 23. A comparison of various public health policy suites. We used the eight imported cases reported in Singapore to trigger the simulation. Policy suites went into effect on day 24 of our 66-day simulations. Suite 1 (cyan): A-class home quarantine for 10 days and reduced public contact; suite 2 (red): wide-scale taking of body temperatures and a restriction on hospital visitations; suite 3 (green): wide-scale taking of body temperatures, a restriction on hospital visitations, and mask wearing by health care workers; suite 4 (pink): public mask wearing and reduced public contact.

considerable flexibility in the model—that is, we believe it can be applied to a wide range of contagious diseases (e.g., influenza, enteroviruses, and HIV/AIDS) that have well-defined epidemic parameters.

7. Acknowledgments

This work was supported in part by the National Science Council, Taiwan, Republic of China under grant NSC 92-2524-S-009-004 and NSC 93-2520-S-009-003.

8. References

[1] Masuda, N., N. Konno, and K. Aihara. 2004. Transmission of severe acute respiratory syndrome in dynamical small-world networks. *Physical Review E* 69:031917.

[2] Newman, M. E. J. 2002. Spread of epidemic disease on networks. *Physical Review E* 66:016128.

[3] Ahmed, E., A. S. Hegazi, and A. S. Elgazzar. 2002. An epidemic model on small-world networks and ring vaccination. *International Journal of Modern Physics C* 13:189-98.

[4] Sirakoulis, G. C., I. Karafyllidis, and A. Thanailakis. 2000. A cellular automaton model for the effects of population movement and vaccination on epidemic propagation. *Ecological Modelling* 133:209-23.

[5] Moore, C., and M. E. J. Newman. 2000. Epidemics and percolation in small-world networks. *Physical Review E* 61:5678- 82.

[6] Newman, M. E. J., I. Jensen, and R. M. Ziff. 2002. Percolation and epidemics in a two-dimensional small world. *Physical Review E* 65:021904.

[7] World Health Organization (WHO). 2003. *WHO consensus document on the epidemiology of severe acute respiratory syndrome (SARS)*. http://www.who.int/csr/sars/en/WHOconsensus.pdf

[8] Kleczkowski, A., and B. T. Grenfell. 1999. Mean-field-type equations for spread of epidemics: The 'small world' model. *Physica A* 274:355-60.

[9] Kuperman, M., and G. Abramson. 2001. Small world effect in an epidemiological model. *Physical Review Letters* 86:2909-12.

[10] Sebastian, B., and C. Hoffmann. 2003. *SARS reference*. http://www.sarsreference.com

[11] Peiris, J. S., S. T. Lai, L. L. Poon, Y. Guan, L. Y. Yam, W. Lim, J. Nicholls, W. K. Yee, W. W. Yan, M. T. Cheung, V. C. Cheng, K. H. Chan, D. N. Tsang, R. W. Yung, T. K. Ng, K. Y. Yuen, and SARS Study Group. 2003. Coronavirus as a possible cause of severe acute respiratory syndrome. *Lancet* 361 (9366): 1319-25.

[12] Boccara, N., and K. Cheong. 1993. Critical-behavior of a probabilistic-automata network Sis model for the spread of an infectious-disease in a population of moving individuals. *Journal of Physics A* 26:3707-17.

[13] Boccara, N., and K. Cheong. 1992. Automata network SIR models for the spread of infectious disease in populations of moving individuals. *Journal of Physics A* 25:2447-61.

[14] Boccara, N., K. Cheong, and M. Oram. 1994. A Probabilistic-automata network epidemic model with births and deaths exhibiting cyclic behavior. *Journal of Physics A* 27:1585-97.

[15] Miramontes, O., and B. Luque. 2002. Dynamical small-world behavior in an epidemical model of mobile individuals. *Physica D* 168:379-85.

[16] Watts, D. J., and S. H. Strogatz. 1998. Collective dynamics of 'small-world' networks. *Nature* 393:440-2.
[17] Newman, M. E. J. 2000. Models of the small world: A review. *Journal of Statistical Physics* 101:819-41.
[18] Wang, X. F., and G. Chen. 2003. Complex networks: Small-world, scale-free and beyond. *IEEE Circuits and Systems Magazine* First Quarter:6-20.
[19] Watts, D. J. 1999. *Small worlds: The dynamics of networks between order and randomness*. Princeton, NJ: Princeton University Press.
[20] Kermack, W. O., and A. G. McKendrick. 1927. Contributions to the mathematical theory of epidemics. *Proceedings of the Royal Society of London* 115:700-21.
[21] Edeletein-Keshet, L. 1988. *Mathematical models in biology*. New York: Random House.
[22] Lipsitch, M., T. Cohen, B. Cooper, J. M. Robins, S. Ma, L. James, G. Gopalakrishna, S. K. Chew, C. C. Tan, M. H. Samore, D. Fisman, and M. Murray. 2003. Transmission dynamics and control of severe acute respiratory syndrome. *Science* 300:1966-70.
[23] Riley, S., C. Fraser, C. A. Donnelly, A. C. Ghani, L. J. Abu-Raddad, A. J. Hedley, G. M. Leung, L. M. Ho, T. H. Lam, T. Q. Thach, P. Chau, K. P. Chan, P. Y. Leung, T. Tsang, W. Ho, K. H. Lee, E. M. C. Lau, N. M. Ferguson, and R. M. Anderson. 2003. Transmission dynamics of the etiological agent of SARS in Hong Kong: Impact of public health interventions. *Science* 300:1961- 66.
[24] Donnelly, C. A., A. C. Ghani, G. M. Leung, A. J. Hedley, C. Fraser, and S. Riley. 2003. Epidemiological determinants of spread of causal agent of severe acute respiratory syndrome in Hong Kong. *Lancet* 361:1761-6.
[25] Chowell, G., P. W. Fenimore, M. A. Castillo-Garsow, and C. Castillo-Chavez. 2003. SARS outbreaks in Ontario, Hong Kong and Singapore: The role of diagnosis and isolation as a control mechanism. *Journal of Theoretical Biology* 224:1-8.
[26] Ng, T. W., G. Turinici, and A. Danchin. 2003. A double epidemic model for the SARS propagation. *BMC Infectious Disease* 3 (19): 1-16.
[27] Anderson, R. M., and R. M. May. 1982. Directly transmitted infections diseases: Control by vaccination. *Science* 215 (4536): 1053-60.
[28] Becker, N. G. 1992. Infectious-diseases of humans: Dynamics and control. *Australian Journal of Public Health* 16:208-9.
[29] Koopman, J. 2004. Modeling infection transmission. *Annual Review of Public Health* 25:303-26.
[30] Ahmed, E., and A. S. Elgazzar. 2001. On some applications of cellular automata. *Physica A* 296:529-38.
[31] Erdös, P., and A. Renyi. 1959. On the evolution of random graphs. *Publication of the Mathematical Institute of the Hungarian Academy of Science* 5:17-60.
[32] Benyoussef, A., N. E. Hafidallah, A. Elkenz, H. Ez-Zahraouy, and M. Loulidi. 2003. Dynamics of HIV infection on 2D cellular automata. *Physica A* 322:506-20.
[33] Yacoubi, S. El, and A. El Jai. 2002. Cellular automata modelling and spreadability. *Mathematical and Computer Modelling* 36:1059-74.
[34] Fuentes, M. A., and M. N. Kuperman. 1999. Cellular automata and epidemiological models with spatial dependence. *Physica A* 267:471-86.
[35] Martins, M. L., G. Ceotto, S. G. Alves, C. C. B. Bufon, J. M. Silva, and F. F. Laranjeira. 2001. A cellular automata model for citrus variegated chlorosis. *Physica A* 295:42-8.
[36] Boccara, N., E. Goles, S. Martinez, and P. Picco. 1993. *Cellular automata and cooperative phenomena*. Dordrecht, The Netherlands: Kluwer Academic.
[37] Ahmed, E., and H. N. Agiza. 1998. On modeling epidemics: Including latency, incubation and variable susceptibility. *Physica A* 253:347-52.
[38] Rapoport, A. 1957. A contribution to the theory of random and biased nets. *Bulletin of Mathematical Biophysics* 19:257- 571.
[39] Milgram, S. 1967. The small world problem. *Psychology Today* 2:60-7.
[40] Comellas, F., and M. Sampels. 2002. Deterministic small-world networks. *Physica A* 309:231-5.
[41] Centers for Disease Control and Prevention (CDC). 2003. *SARS: Frequently asked questions*. http://www.cdc.gov/mmwr/mguide_sars.html
[42] CDC. 2003. Update: SARS—Singapore. *Morbidity and Mortality Weekly Report* 52 (18): 405-11.
[43] CDC. 2003. Cluster of SARS cases among protected health-care workers—Toronto, Canada. *Morbidity and Mortality Weekly Report* 52 (19): 433-6.
[44] CDC. 2003. SARS—Taiwan. *Morbidity and Mortality Weekly Report* 52 (20): 461-6.
[45] CDC. 2003. Update: SARS—Toronto, Canada. *Morbidity and Mortality Weekly Report* 52 (23): 547-50.
[46] CDC. 2003. Update: SARS—Worldwide and U.S. *Morbidity and Mortality Weekly Report* 52 (28): 664-5.
[47] CDC. 2003. Use of quarantine to prevent transmission of SARS—Taiwan. *Morbidity and Mortality Weekly Report* 52 (29): 680-3.
[48] CDC. 2003. Revised U.S. surveillance case definition for severe acute respiratory syndrome (SARS) and update on SARS cases—United States and worldwide. *Morbidity and Mortality Weekly Report* 52 (49): 1202-6.

Chung-Yuan Huang *is* ****POSITION?**** *in the Department of Computer and Information Science at National Chiao Tung University, Taiwan and* ****POSITION?**** *in the Department of Computer Science and Information Engineering at Yuanpei Institute of Science and Technology, Taiwan, Republic of China.*

Chuen-Tsai Sun *is* ****POSITION?**** *in the Department of Computer and Information Science at National Chiao Tung University, Taiwan, Republic of China.*

Ji-Lung Hsieh *is* ****POSITION?**** *in the Department of Computer and Information Science at National Chiao Tung University, Taiwan, Republic of China.*

Yi-Ming Arthur Chen *is* ****POSITION?**** *at the Institute of Public Health, National Yang-Ming University, Taiwan, Republic of China.*

Holin Lin *is* ****POSITION?**** *in the Department of Sociology at National Taiwan University, Taiwan, Republic of China.*